



No. 81 – September 1995

TELESCOPES AND INSTRUMENTATION

News from Paranal and Current Status of VLT Construction

M. TARENGHI, ESO

On Sunday, 30 July 1995, at 1.15 hours local time, an earthquake shook northern Chile near the city of Antofagasta. The earthquake was estimated to be of magnitude 7.8 on the Richter scale. Most damage was concentrated around Antofagasta. The Paranal Observatory was also affected although no severe damage occurred as the structures under construction resisted as foreseen to the violence of the vibrations. A week later the ESO photographic team visited the site; their photographs which are shown here record the current status of construction.



Figure 1.

Figure 1 shows Unit Telescope No. 1 with its foundation complete and the fixed part of the enclosure's steel structure already in place. In Figure 2, detail of the Nasmyth Access Platform is visible. Figure 3 shows the inner part of

Figure 2 shows a close-up view of the Nasmyth Access Platform, a complex steel structure with multiple levels and walkways, built around the telescope's enclosure. The structure is made of dark metal beams and plates, with a curved walkway visible. The background shows a clear blue sky and the desert landscape.



Figure 2.

telescope No. 1 with the inner and outer rings that will form the base for the telescope structure. The work on telescopes 2, 3 and 4 is proceeding as planned. Figure 4 shows the advanced stage of telescope No. 2 whose concrete foundation will be ready towards the end of October. In the background one can see work commencing on the foundations for telescope No. 4.

The interferometry complex has progressed considerably during the course of the last months. Figure 5 shows the

building that will be used as the laboratory to combine the beams both in the coherent and incoherent way. On the right below ground level the interferometric

tunnel is visible. Progress has also been made on the construction of the steel structure of the control buildings seen in Figures 6 and 7. (Photographs by H. Zodet)

Figure 4.



Figure 3.



Figure 5.

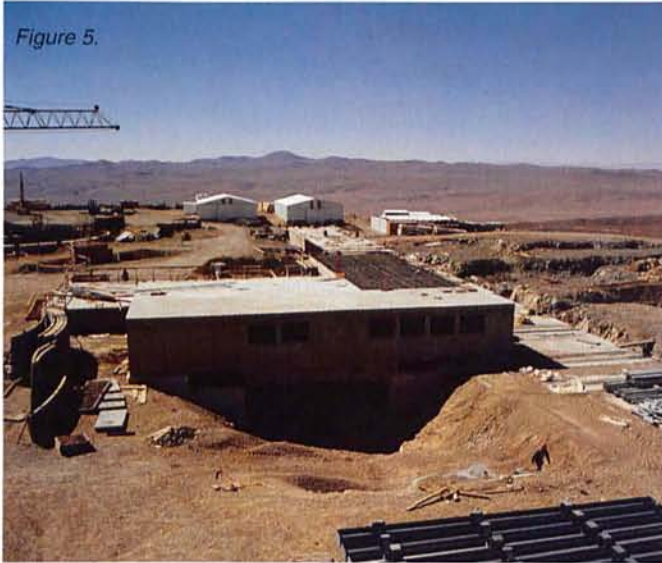


Figure 7.

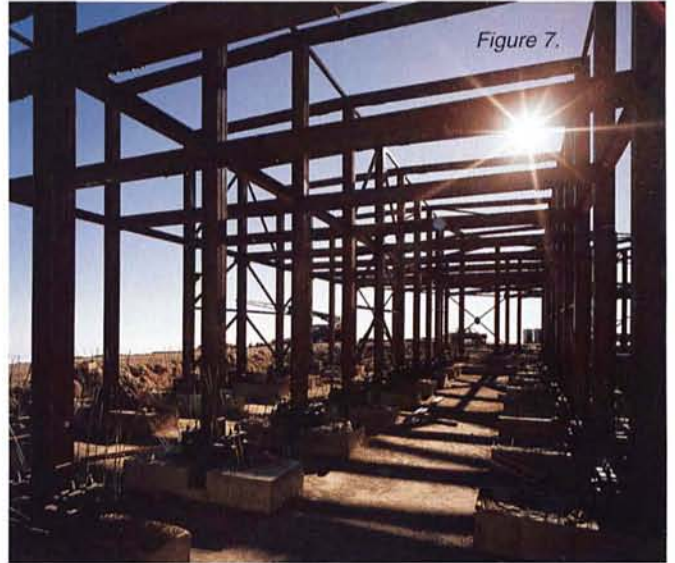


Figure 6.



ESO Donates DM 100,000 for Reconstruction Work After Earthquake in Northern Chile



On Sunday, July 30, at 1.15 hours, the Antofagasta region was struck by an earthquake, reaching 7.8 on the Richter Scale. Three people died and more than 130 houses and buildings were damaged beyond repair. The port also suffered damage.

In an act of solidarity with the local community and its authorities, ESO immediately decided to donate 25 million Pesos (about 100,000 DM) towards the reconstruction work, and on August 7, a cheque was handed over to the Intendente for the II region, Mr. Cesar Castillo, by Daniel Hofstadt of ESO Chile.

C. Madsen

Photographer: H. Zodet

News from the Secondary Mirror Units

D. Enard, ESO

Can a talented writer make a breathtaking novel out of the M2 Unit story? Well, . . . sounds a priori difficult but . . .

The ink of issue 76 (June 1994) of *The Messenger*, where I wrote a short article relating the effective start of the M2 Units contract, was not fully dried that ESO received a "red flag report" mentioning quite unexpected difficulties with the supplier of the Silicon Carbide mirror blanks who suddenly and for quite

unclear reasons withdraw from his previous commitment. After three months of stormy discussions, negotiations, looking for alternatives, moving forward, backward, etc., it was finally decided to select DORNIER as the new contractor and an ATP (Authorisation To Proceed) was signed beginning of September, intended originally for the delivery of 4 electromechanical units and 4 Silicon Carbide and one Beryllium mirrors.

After negotiations the new contract was finally signed in November 1994. The scope of the contract was reduced to the delivery of 4 electromechanical units and to one Beryllium mirror only, the three remaining mirrors having to be contracted separately at a later stage. The reason for this delayed procurement was essentially the very uncertain situation of the light-weight mirror market, in particular with respect to prices and guaranteed delivery. This situation is essentially due to the opening of the Eastern countries, which can now deliver high-tech products at very competitive prices, and simultaneously the collapse of military orders in the US with, as consequences, the declassification of certain technologies on the positive side but also, on the negative side, a financial fragility and uncertain future of potential suppliers.

At the moment the more promising technology in terms of cost and performance still seems to be Silicon Carbide although there is a fierce competition with Beryllium which tends to become more affordable than in the past, in part for the reasons mentioned above. The well-known potential drawback of Beryllium is the risk of deformation over long periods of time. However, important progress has been made in the processing of Beryllium in particular with the use of HIP technology (Hot Isostatic Pressing) and the development of sophisticated annealing procedures which



Figure 1: First machining of the Beryllium mirror at LORAL on July 6. Second from left: Marc Cayrel (REOSC), P. Dierickx and A. Michel (ESO), Bob Langenbach (LORAL).

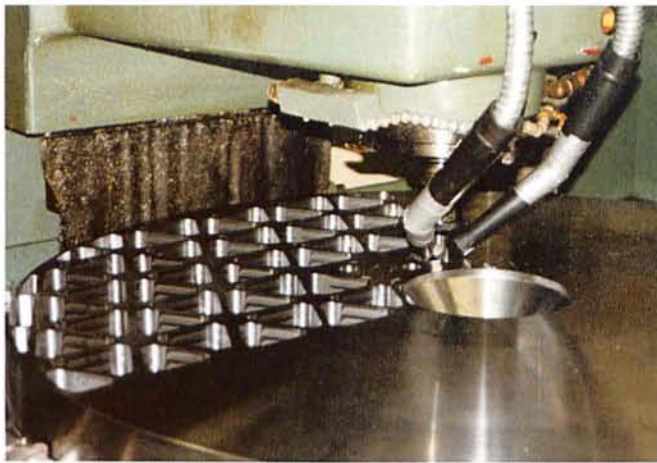


Figure 2: Close up on the Beryllium mirror during machining. Because of its potential toxicity, machining of Beryllium requires some safety measures: the two pipes on each side of the tool are connected to a sucking device which recuperates the metal chips as well as possible toxic vapours.

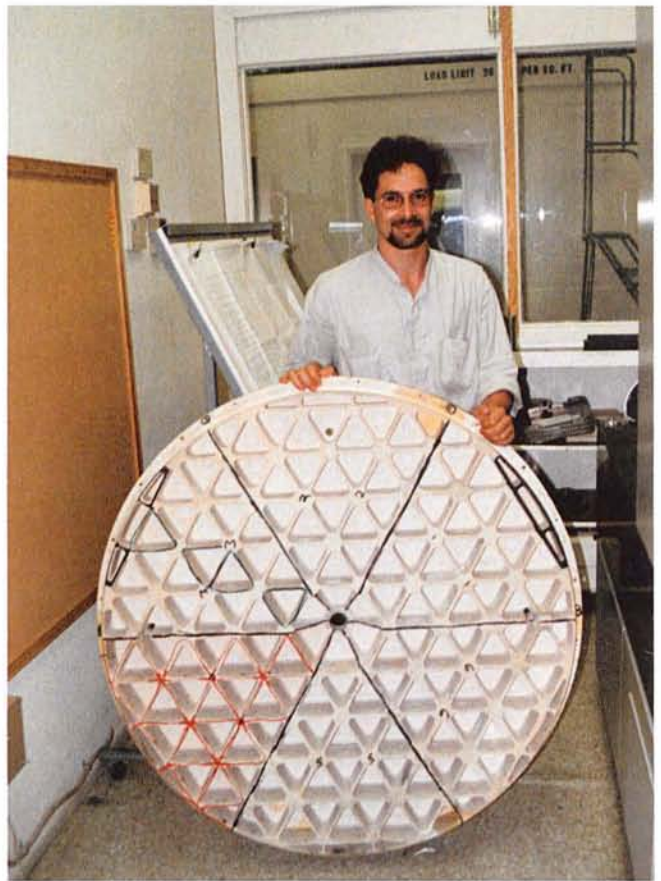


Figure 3: This plastic model has been realised to verify the machine tool programme before machining the real Beryllium piece. Standing: Marc Cayrel, responsible at REOSC for the M2 mirror programme.

make nowadays Beryllium an excellent mirror material even for cryogenic applications.

The reason to select Beryllium for the first unit is simply the relative security that a good mirror will be

available on time for the first light of the VLT.

The VLT M2 Beryllium mirror is produced out of a solid piece produced by Brush-Wellmann in the US through the HIP process. The machining is contracted to LORAL and to TINSLEY for the fine turning of the surface according to the aspheric shape. The mirror is then sent back to LORAL for the deposition of a nickel coating before final grinding and polishing performed by REOSC.

The design of the Electromechanical Unit is progressing well. The Final Design Review is expected in November after a series of tests on the Chopper breadboard. This breadboard will later be converted into the final chopper unit to the extent that the tests are successful. The highly demanding dynamic performance required from the M2 units makes this test very critical and ESO looks (nervously) forward for the first results in September 1995.

E-mail address:
D. Enard, denard@eso.org



Figure 4: CAD picture of the M2 Unit. The chopper stage is located at the bottom. It is equipped with a dynamically balancing system, intended to compensate the reaction forces which could cause oscillation of the electromechanical assembly.

The VLT Control Software – Status Report

G. RAFFI, ESO-Garching

Introduction

The VLT control software consists of all the software, which will be used to directly control the VLT Observatory and associated instrumentation. This is now in the implementation phase, performed to a large extent directly by ESO staff in the VLT software group, but also by Consortia of Institutes responsible for some ESO instruments and by Contractors who implement some of the telescope subsystems.

The main foundation body for the VLT control software, called VLT common software, has already been implemented at about 90% by now. It is used across all computers of the VLT observatory (telescopes and instruments) and is designed, implemented and maintained by the VLT software group. The group is also responsible for monitoring software developed outside ESO and for later integration into the VLT control software at the VLT Observatory.

Starting with this *Messenger* issue, regular reports on the VLT control software will be given in *The Messenger*. The first contribution, just after this Status Report, is an article on the Real Time display software.

VLT Common Software

The general architecture of the VLT control system consists of a fully distributed system based on a number of workstations and microprocessors, called LCUs (Local Control Units). There will be about 40 workstations and 150 LCUs in the complete VLT and instrumentation configuration. This complies with the VLT control system architecture, as defined for the VLT project by the Electronics Department.

The VLT common software consists of a layer of software over the UNIX operating system, in the case of workstations and on top of the VxWorks operating system, for the LCU microprocessors.

The main Packages in the VLT common software are: LCC (LCU Common software). It works on LCUs over VxWorks and is completed by a set of drivers for the ESO standard cards and a user interface (GUI) on the host workstation. It is the common platform for all the LCUs of the VLT and instruments. A motor library, dealing with the VLT standard control cards is also contained in this software. Test and debugging tools are provided.

CCS (Central Control Software). It is a layer of software built on top of a commercial system (RTAP, Real Time Application Platform by Hewlett-Packard), which provides a real-time database, runnable on several UNIX platforms. It contains also a tool to assist in the implementation of user interfaces (Panel editor).

HOS (High level Operation Software). It consists of a set of high-level tools to provide support for operators and astronomers, also in the preparation phase of observing runs.

Additionally there is a library, which forms what is called the Instrumentation common software and is specific to instrumentation applications.

VLT Common Software Releases

The VLT common software is used in the whole VLT programme, telescope and instruments, by ESO staff, Contractors and Consortia. It is also the basis for the NTT upgrade project.

Therefore, the VLT software group has been supporting for one and a half year a system of releases of this software, which is by now distributed to about 15 sites, both internal and external to ESO and runs on both HP (HP-UX) and SUN (Solaris 2) platforms. The next release will be distributed externally at the end of August 1995.

The VLT common software has a size of about 400,000 lines of code (including code, comments and test procedures), mostly written in C, but C++ is on the increase and Tcl/Tk procedures are also present.

Together with all this goes also a relevant Maintenance activity, supported by a system of SPRs (Software Problem Reports or Change requests). The level of confidence in the capabilities and quality of the VLT common software is quite high at this stage. This results from all the implementations and tests done by the NTT team for the NTT Upgrade project (see also separate section in *The Messenger*) and by other field tests at La Silla, like the one carried out with a CCD prototype in January 1995.

VLT Control Software for Telescopes and Instruments

This is the main part of the VLT software and emphasis is shifting towards it, as more and more design work gets completed. Implementation has started within the VLT software group in

several areas, like telescope subsystems, telescope co-ordination, CCDs, ISAAC prototypes.

The first internal milestone of the Telescope Control System software (TCS) will be reached in August, with integration of co-ordination software and subsystems. This is actually a joint venture between the VLT and the NTT upgrade teams, so that most of the software will be the same.

The next major milestone for TCS is then coming at the end of the year, when TCS has to get ready for tests in Milan next year.

For what concerns instrumentation and detector software, the scientific CCD software will reach its first milestone, after the January 1995 prototype tests, in August. Instrumentation software starts to be implemented also in ESO, taking advantage of the INS common software. In particular prototypes for the ISAAC detector software are being developed, while the UVES software is still in the design phase. Collaboration with the NTT team, upgrading now the EMMI software, allows early verification and potential sharing of software.

Other Software for the VLT

Interfaces with the off-line software, which is also essential to run the whole VLT observations cycle and will be developed by the Data Management Division of ESO, are already partly defined and partly still in the definition phase. This includes interfaces to MIDAS, Archive, Scheduler and Catalogues. The VLT software group participates also in the activities of the On Line Data Flow working group.

The software developed outside ESO for the VLT by Consortia and Contractors is not mentioned in detail here.

VLT Control Software Trends

A set of new tools in the CCS software (Database Loader, Extended CCS, Event Handler, Class Browser) support an object-oriented design and implementation of the VLT software (workstation part). The VLT control software projects developed in ESO at the moment make use already of such tools.

A kernel of software, called CCS-lite, has been isolated in the CCS software. It consists of Panel editor, Sequencer, message system, error and logging system and database access to LCU databases.

CCS-lite does not require HP RTAP and therefore does not allow to access the workstation based real-time database. It allows though to easily implement user interfaces to LCU software, providing access to LCU databases and support at the workstation level for passing messages, errors and logs. It represents also an easily portable platform to any users, who will be able to prepare an Observing programme ahead of time on a generic UNIX workstation.

Some developments, like the Real time display, although part of the VLT control software, have been implemented in a fully portable way and can run completely independent of the VLT software (see following article).

Documentation and Standards

A complete set of specifications and user manuals exists for the VLT software

and for the VLT common software in particular.

In spite of the large number of documents, there exist obvious "access roads" to documentation. So if you are interested in instrumentation software, you should simply start reading one document: VLT Instrumentation software specification. (Please refer to latest issue of 12/4/95.)

If instead the point of interest is telescope subsystems, the access specification is: VLT software – Telescope Control system functional specification.

These two documents can also be used as references to any other documentation, if deeper understanding is required.

The general requirements, standards and rules for this software have been fixed some time ago (although there is a constant evolution in the project) by the VLT software group.

All documents are available from the VLT Archive or directly via the ESO home page of the World Wide Web (main documents).

Meeting with Consortia and Contractors

A two-day meeting on the VLT control software was held at ESO on June 19–20, 1995. Software representatives of about 10 external Consortia and Contractors were present. The meeting was organised around a number of tutorials and demonstrations, as most of the software comes with a set of auxiliary tools and user interfaces, to facilitate development.

For more information on the VLT software please use the ESO home page in the WWW. Should you have additional questions, you can contact by e-mail either graffi@eso.org or other members of the VLT software group.

The VLT Real Time Display Software

T. HERLIN, A. BRIGHTON, P. BIEREICHEL, ESO

Introduction

The VLT will contain a large number of technical CCD's, which will be used for guiding and slit-viewing cameras requiring real-time display facilities. The frequency of image display from these image sources can be several Hz, for example, while performing tracking. For scientific detectors, real-time display capability is equally important. In particular, requirements for infrared detectors have been a driving force in specifying the functionality for a real-time display system.

The Real Time Display (RTD) software was developed in order to support image display in real-time on the VLT. The RTD software provides a tool for users to display video like images from a camera or detector as fast as possible on a workstation or X-terminal. The RTD is implemented as a package providing a widget and library. It is designed to be a building block, adding display capabilities to dedicated VLT applications in areas such as telescope and instrument control.

The intention of RTD is *not* to provide the image processing functionality already existing with image processing packages such as MIDAS. Functional overlapping with image processing systems is kept to a minimum and confined to the area of on-line operations.

Although it is part of the VLT control software, the RTD is an independent software package and does not require any other VLT software components, external packages, such as MIDAS or any commercial products.

Functionality

The core of RTD is an image display widget which supports two image sources: cameras and FITS files. The *camera* is either a technical CCD or scientific detector, which provides the image data in shared memory. The RTD widget is notified via an image event mechanism by the *camera* that a new image is available. See below for more about real-time images.

Figure 1 shows a typical screen layout when working with the RTD widget. The application shown was designed for demonstration purposes and shows an image loaded from a FITS file.

The user can change the magnification of the displayed image, zooming in to get a close-up view of a section of the image or zooming out to get an overall view of a large image. A panning window supports navigation on the image and a zoom window enables the targeting of a single pixel.

The RTD widget supports a basic set of colour scaling algorithms: linear,

square-root, logarithmic and histogram equalisation. MIDAS compatible colour maps are supported by the RTD widget as well as the MIDAS intensity transfer tables.

The colours can be manipulated by a colour bar rotating the colour map or changing the slope of the intensity via mouse interaction. The colour distribution can be changed by either manually setting the cut-levels or using automatic cut-level calculation.

The widget supports line graphics so that the user can overlay markers and text on the image. This might be used, for example, to identify interesting areas around a star. Standard line graphic components such as line, circle and text are available and can be drawn interactively on the image. Line graphic attributes such as line width, colour, filling, font, etc. can be set by the user via buttons and menus. In addition to the interactive line graphics, a programmatic interface is available to support overlaying of more complex line graphics, such as star maps taken from a catalogue.

Pixel query operations are supported at various levels:

- get and/or display the value of the pixel directly under the mouse.
- get and/or display a table of pixel values surrounding the pixel directly under the mouse.

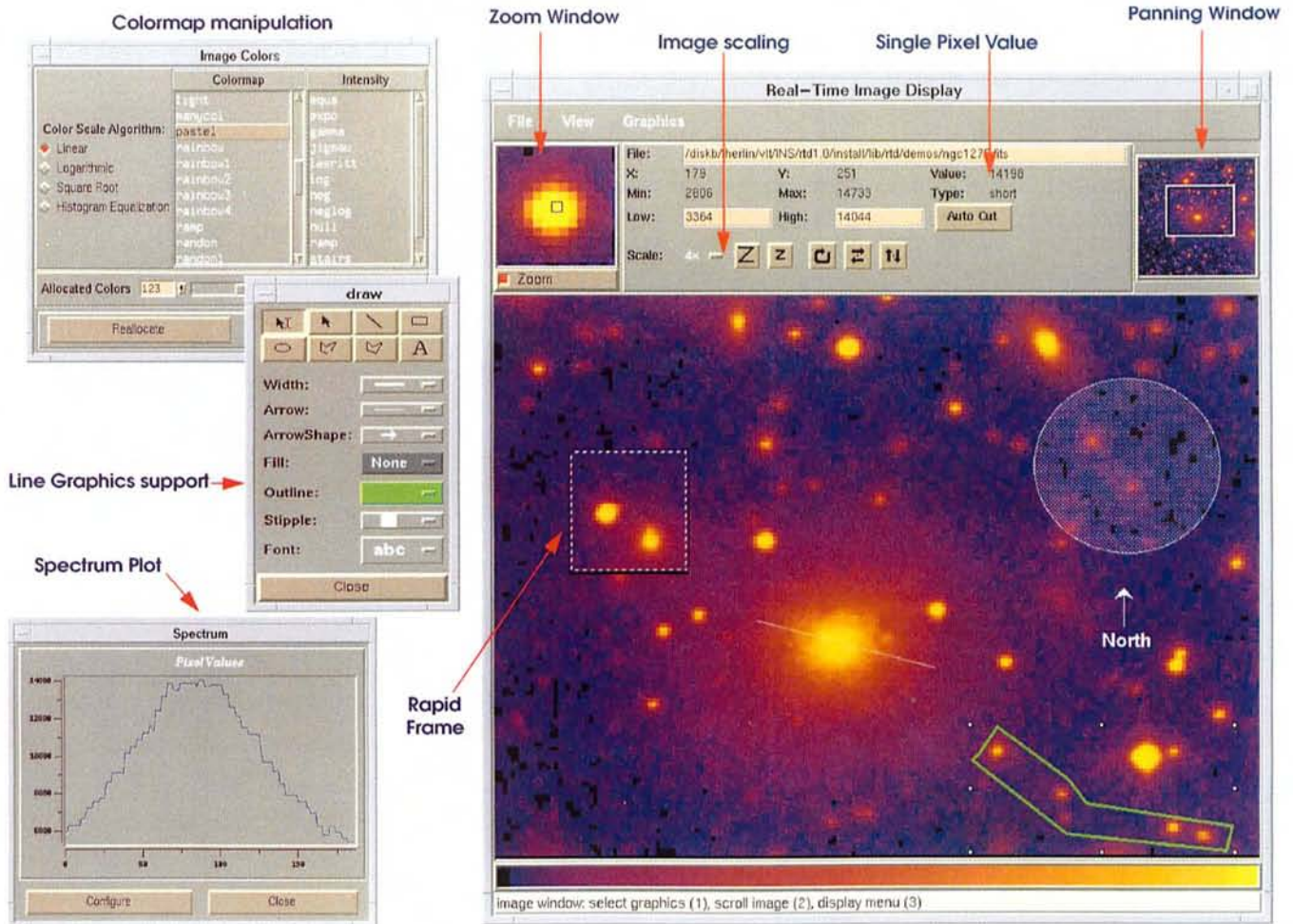


Figure 1.

Another level of pixel value inspection is supported by a spectrum plot along a *cut* line drawn interactively on the image. The pixel values are displayed in a separate graph window.

The RTD widget provides a library with basic image handling functionality referred to as the Real Time Image (RTI) library. In addition to basic image handling algorithms, the RTI library provides a data access framework for application developers supported by a well-defined application programming interface (API). This enables developers to contribute to and extend the image handling capabilities of the library.

Real Time Images

In order to use the RTD widget for real-time, an image event mechanism is provided by the RTD software. The image event is sent by the subsystem controlling the *camera* device e.g. CCD subsystem or infrared detector control software. The image event contains information about the image, for example, data-type, size and the reference to the shared memory location for the image data. The event is sent to an RTD server process which keeps a list of RTD applications registered for notification of a specific 'camera'. If there is a match, the image event

is dispatched to the corresponding RTD application.

Figure 2. shows a diagram of the image event architecture.

The advantage of using this decoupled approach is that the *camera* subsystems and the RTD applications become independent of each other and several RTD applications can attach to the same camera source.

The RTD server will also (currently not implemented) support eavesdropping which is the multi-casting of images to remote machines, which could be used, for example, for remote observing. For eavesdropping issues, such as network bandwidth and image compression techniques, e.g. H-transform will be investigated.

Updating images in real-time places a

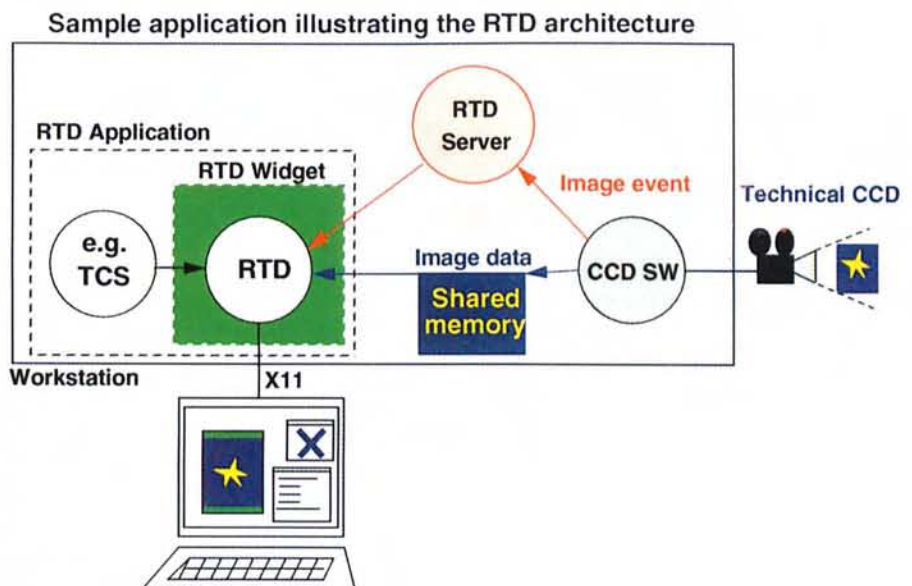


Figure 2.

high demand on the CPU and the network. For some images the variation between exposures is only interesting in a small area. In this case, a *rapid frame* can assist the selection of a specific area, for example around a star. This typically small frame can be updated faster than the rest of the image while the user still sees the complete picture. By using *rapid frames*, an image update frequency of more than 10 Hz is expected to be possible. Detailed performance measurements will be done based on the first release of RTD.

Implementation

The RTD widget is implemented as a Tcl/Tk (Tk 4.0) widget using C++. The RTI library is also implemented in C++ but as an independent library. In order to support fast application development with the RTD widget, a large set of [incr Tcl] widget classes is provided for managing, among other things, a zoom window, a panning window and a line graphics tool-box.

Although Tcl/Tk code is interpreted, the performance of the RTD widget when updating images in real-time is not degraded. This is due to the fact that all image related operations are implemented entirely in C/C++. Only the user interface parts of the software, such as buttons and menus are actually interpreted at run-time.

The image event mechanism uses standard UNIX IPC and image data is passed using shared memory as recommended by the real time extension standard POSIX.4.

The display on X-terminals is supported, although for very fast image display frequencies, workstations are recommended. In addition, on workstations the X11R5 extension for X Shared Memory is supported, giving the final boost for passing the scaled pixmap to the X-Server.

The software has been ported and tested on the following workstation platforms: HP (HP-UX) and Sun (SunOS & Solaris 2.3).

For RTD application development, the VLT Panel Editor can be used to develop control panels using the RTD widget. The VLT Panel Editor supports the interactive placement of GUI components and generates panels that comply with the ESO VLT common conventions for GUI development.

Availability

The RTD software is part of the VLT control software and the first release is available on the July '95 release of the VLT SW. For people interested and not receiving the VLT control software, the RTD user manual is accessible on anonymous ftp via the following WWW reference: ftp://te1.hq.eso.org/vlt/pub/doc/rtd_sum1.0.ps.gz.

For more information on the RTD software please contact: Thomas Herlin – ESO VLT SW group preferably via e-mail: therlin@eso.org.



(With this periodically compiled collection of short notes, the NTT Team intends to keep the community informed about changes in performance, configuration, and operation of the NTT and its subsystems.)

Big Bang Rescheduled

Because of a possible uncertainty in the manpower available in 1996 for the implementation of the new VLT-like control system, the date when the implementation will start has been shifted from April 1 to July 1, 1996. This means that the operation of the NTT will continue unchanged through June 30. Final adjustments will take place after field tests in December 1995 (Telescope Control System) and February 1996 (EMMI control software) of two critical components. Observers who might get time after June 30 will be informed about the allocation of observing time, if any, after the evaluation of the test results. This change in schedule does not seriously compromise the NTT's ability to provide useful feedback to the VLT project.

Further announcements will be made in *The Messenger* and on the World Wide Web (see below).

The NTT on the World Wide Web

As part of ESO's efforts to make more extensive use of the World Wide Web to inform the scientific community (which was strongly encouraged by the Users

Committee), NTT pages are under development. By the time of publication of this issue of *The Messenger*, they should be accessible from the ESO home page (<http://http.hq.eso.org/eso-homepage.html>). In addition to general information about the NTT and the NTT Upgrade Project, any up-to-date announcements will from now on be made on the Web. The previously maintained electronic bulletin board will be discontinued. The Information Desk of the general ESO pages can also be used for inquiries with the NTT Team (e-mail can as before be sent also directly to ntt@eso.org).

Update of EMMI/SUSI Manual

A major revision is currently under way of the EMMI/SUSI manual. In order to let prospective applicants for observing time with the NTT in Period 57 take advantage of the progress made, intermediate versions will be made available electronically. Details will be provided on WWW (see above).

Automatic Guide Star Selection

The Data Handling and Observation Support Group has installed the HST

guide star catalog and a new server on one of the workstations in the NTT building. The performance is for a number of reasons vastly superior to the previous temporary solution which depended on STARGAT in Garching. Guide stars are now on a routine basis automatically supplied for every new preset. First attempts to acquire also the guide star in a fully automatic way with the guide probe have been very successful. Since the light of the guide stars is via a beam splitter also used for parallel image analysis, efforts to adjust the exposure times with the image analyser according to the magnitude of the star are under way.

Graphical Log of Image Analysis Data

With the implementation of the cyclic image analysis in parallel mode, the self-diagnosing capabilities of the NTT can now be much better exploited. In order to enable also Visiting Astronomers to keep track of the performance of the telescope, tools have been developed to plot individual aberrations as measured before and after the setting of the forces versus time. In addition, the level to which aberrations should ideally be corrected is indicated.

This should help to make the results of the image analyses easier to interpret, a wish expressed by several observers. The night assistants start the system at the beginning of every night.

Field Test of Major Component of New Control System

In May, another major field test of the new VLT-like control system was performed. With the many motorised functions of the adapter, it was a major test also of the first release of the VLT motor library. Again, no fundamental problem was found. However, further tests have to be performed on side A (IRSPEC/SUSI) to fulfil all objectives.

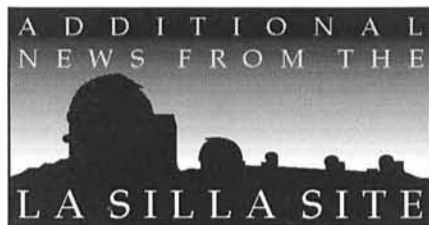
An important logistical result has been that, with the necessary careful preparation, it is feasible that such tests can be performed by on-site staff who have not been directly involved in the writing of the code. A necessary requirement was, of course, the availability of the high-speed link between Garching and La Silla. Due to the time difference between Chile and Germany, the test engineers at La Silla could every morning resume their work with a new version of the software which had been further debugged in Garching on the basis of the previous day's test results.

This is an important and encouraging conclusion for the commissioning and operation of the VLT.

Digital Sky Survey On Line

Thanks to the help of the Observation Support and Data Handling Group, the Digital Sky Survey prepared by the Space Telescope Science Institute is now available on line to remote observers in Garching. The same service will soon be offered to NTT observers at La Silla, too. It should prove to be very useful for the preparation of observations (astrometry, finding charts) as well as for the comparison with observations of a field at an earlier epoch.

The NTT Team
e-mail address: ntt@eso.org



CASPEC Thorium-Argon Atlas in the 3050–3650 Å Region

L. PASQUINI and L. ACHMAD

The CASPEC spectrograph has been in use for more than 10 years at the 3.6-m telescope at La Silla. With the implementation of the Blue Cross-disperser (Pasquini and Gilliotte, 1992) and the advent of new detectors, CASPEC has reached very good capabilities in the blue-UV range, and the demand for its use at these spectral regions has rapidly grown.

Because the existing CASPEC Thorium-Argon Atlas (D'Odorico et al., 1987) extends only to 3600 Å with the 31.6 lines/mm echelle and to 3400 Å with the 52

lines/mm echelle, an extension was required to provide the users with a suitable reference for working in the UV. A new atlas has thus been prepared to fill this gap. The 31.6 lines/mm echelle was used in combination with the Long Camera and the new 1K Tektronix CCD (ESO #37). A new line list is now available, which extends to 3060 Å, and is implemented in the MIDAS package. The present Atlas is intended to serve CASPEC users, and we are confident that it may also be helpful for observers using different instrumentation. Paper

copies are available at the La Silla Observatory (Astronomy Secretary) and at the Headquarters in Garching (Section Visiting Astronomers). The Atlas is also available in the WWW ESO/La Silla home page (Documentation/Others section).

References

- D'Odorico, S., Ghigo, M., Ponz, D., 1987: 'An Atlas of the Thorium Argon Spectrum for the ESO Echelle Spectrograph in the $\lambda\lambda$ 3400–9000 Å Region', ESO.
Pasquini, L., Gilliotte, A., 1992: 'CASPEC Improvements' *The Messenger* 71, 54.

Rotating Half Wave Plate for EFOSC1 Refurbished

H. SCHWARZ and S. GUIARD

The polarimetric mode of EFOSC1 at the 3.6-m telescope has been made more sophisticated by the addition of a rotatable super-achromatic half wave plate (HWP). In addition to imaging polarimetry, it is now possible to do spectropolarimetry of extended objects by using a MOS mask with a series of 19" long slitlets, spaced 21" apart along a direction perpendicular to the dispersion. For objects larger than 20", two images have to be taken with a telescope shift of 20" in between, for smaller objects, one image suffices since the source falls entirely within one slitlet. Two images per telescope position have to be taken with a 22.5° rotation of the HWP for the second

image. These images yield two orthogonally polarised signals each, thus providing four signals from which the polarimetric and intensity information can be derived. Since only three are needed, there is even some redundancy. Twice the mean of the sum of all four images gives the intensity of the source. No instrument rotation is necessary now.

The acquisition of objects for both imaging and spectropolarimetry has become faster, because there is no longer the need to re-acquire the objects after rotating the instrument. By using two special masks, mounting the Wollaston polarising prism in the filter wheel, and the necessary filters and grisms in the grism

wheel, both imaging and spectropolarimetry can be done with one setup of EFOSC1. Masks have been prepared with coronagraphic spots, allowing coronagraphic polarimetry to be done. By letting the HWP rotate continuously, flat-fielding is made easier too.

Recently, this super-achromatic half wave plate for EFOSC1 was refurbished by Halle, to remove a 40" wedge on the faces of the plate, and to improve the optical quality of the surfaces. This wedge produced image motion of about 100 μ m on the CCD when rotating the HWP, making data reduction more difficult. The wedge is now less than 2" and the optical quality about $\lambda/6$ over the surface.

Commissioning of the refurbished HWP was done during the EFOSC1 set-up night of 18 July 1995. Image motion on rotation, ghosts and user friendliness of the control programme were looked at. Total image movement on rotating the plate through 22.5° is less than 0.1 pixel, and when rotating the HWP continuously the resulting image of a pinhole is $1.39''$ FWHM compared to $1.37''$ when stationary. So the above-mentioned image motion is virtually completely eliminated. Ghosts have been measured on pinhole images in the corners and centre of the CCD. For a level of about 25,000 ADUs in the main images, the ghosts were 3×10^{-4} in the corners, and 9×10^{-4} in the centre. These are acceptable values when compared with typical ghosts produced by high-quality optical filters.

The control programme runs on a PC and is very easy to use; start up is done automatically by switching on the PC (or by resetting it), and the functions of the HWP are controlled by a few softkeys. The plate can be put in or out of the beam, it can be made to rotate continuously for flatfielding, it can be set to any position angle or stepped in fixed steps. A concise operating manual is provided.

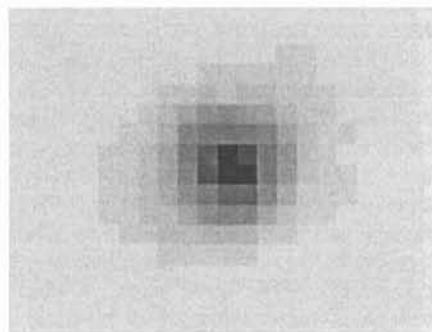
The rotating super achromatic HWP is offered as an option on EFOSC1 from now on.

Superb Seeing on the 2.2-m Telescope with IRAC2

C. LIDMAN

On rare occasions the seeing monitor at La Silla reports seeing below $0.3''$. The first half of the night on May 9, 1995, was such an occasion.

The following image shows a star imaged for 30 seconds at K ($2.2 \mu\text{m}$) with IRAC2b on the 2.2-m during the same night. The pixel scale is $0.14''$, the smallest available with IRAC2b, and the FWHM of the image is an incredible $0.24''$. At this wavelength, Rayleigh's criterion is satisfied with an angular separation of $0.24''$. The observer notes that due to guiding errors it was very difficult



to obtain round images in such excellent seeing.

Photometry with EFOSC2

A piece of metal fell on the EFOSC2 collimator on April 20, 1995. As a result of that incident, photometry is not possible in about 1/8 of the chip on the bottom left corner, and possibly more. There may also be a possible problem with scattered light from bright objects that fall on this

black spot. Some preliminary tests were performed recently which seem to indicate that flatfielding can be reasonably well achieved. A new collimator has been ordered and should be available by October 1995.

New Autoguider at the 1.52-m

C. OLIVEIRA

A new autoguider has been successfully installed and tested on the ESO 1.52-m telescope. Originally developed at Kitt Peak National Observatory and controlled by a PC, it has been interfaced to the ESO 1.52-m telescope control system. This autoguider incorporates a

CCD camera and a Gaussian centring algorithm that determines the position of the guide star with respect to the cross hair. The field of view for the guider camera is $4.1' \times 2.5'$. User-controlled integration times can be set from one second to one minute.

During the autoguider tests, successful guiding was possible for stars as faint as $m_v = 18$ (during bright time). Some simple guidelines on how to operate the autoguider can be found in the update of the B&C manual or in the control room of the ESO 1.52-m telescope.

Satellite Pictures Available in the "Meteomonitor" Environment

J. MENDEZ

Satellite pictures are now included in the "Meteomonitor" programme. The daily 18:00 UTC infrared and visible images of the Pacific Ocean and Chile from the US GOES7 satellite are avail-

able. To visualise them, select the option "h", and then "i" or "v" for the infrared or the visible one. The infrared South America picture (coming from GOESE and updated every 6 hours)

can be obtained by pressing "s". A movie corresponding to the last 30 pictures can be displayed with the option "m".

The Last Trip of the ESO GPO

G. IHLE

The 14th of June, 1995, the GPO started its final trip from La Silla to a storage place in our office in Vitacura.

This could be a dry obituary of a

telescope that played a role in ESO's history, but reflects the development of the organisation's astronomy and its instrumentation.

The GPO (Grand Prism Objectif) was designed by Prof. Ch. Fehrenbach as a double astrograph. Twin parallel tubes, each of 4 metre focal length, were

mounted on a cradle and fitted with a 40-cm diameter doublet objective lenses. The observer guided through one of the tubes and exposed through the other one. A specially developed prism by Fehrenbach could be mounted on top of the objective. A second exposure after a 180 degrees rotation of the prism allowed determination of radial velocities to an accuracy of ~ 5 km/sec.

The GPO was the twin of another one installed in Haute-Provence Observatory and firstly introduced by its previous owner, Marseille Observatory, in Zeekoegat (South Africa) in the middle of 1961. The telescope was extensively used for the ESO site testing in South Africa in combination with research astronomical programmes until the end of 1965.

After the astrograph was dismantled, the mechanical parts were sent to Chile, where they were stored during 1966 and 1967 while the optical parts were taken to France for overhaul. During May 1968, the telescope was erected and

assembled at La Silla, beginning its routine job in mid-June of that year. The telescope was used by Marseille astronomers until the end of April 1969. The 1st of May, 1969, ESO took over the control of the GPO with staff astronomers observations. From October that year the telescope was given to visiting astronomers programmes. In 1992, a programme from a French consortium led by the Institut d'Astrophysique de Paris combined a 40-cm telescope tube with an array of 16 Thomson CCDs mounted in the GPO structure used as the drive unit. This programme, known as the EROS experiment, aimed at searching for halo dark matter via gravitational microlensing of visible stars in the Magellanic Clouds and the Galactic bulge, and last until the final days of the GPO.

The first plate was taken in Zeekoegat on July 18th, 1961, at 22 h local time by Ms. and Mr. Dufлот, pointing at ϵ Scuti with an exposure time of 2.5 minutes. Com-

ments: "un peu surexposé". No indication of the emulsion used, most likely IlaO. No less than 15,000 plates later, on June 4th, 1995, astronomers O. Hainaut and C. Coutures exposed during 45 minutes a IIIaJ plate targeted on the SMC, towards the end of the morning twilight. That is the last plate taken.

The actual site of the GPO and its dome will soon host "MARLY-EROS II" which will pursue the EROS experiment. This new project will use the MARLY 1-m telescope together with a 16-wide-field CCD-cameras array (2000 \times 2000). The telescope is already operational at Observatoire de Haute-Provence, and the CCDs array is under final tests at CEA-Saclay. First observations should start next October.

E-mail addresses for contributions to, and inquiries about this section:
pbouchet@eso.org; rgedel@eso.org;
clidman@eso.org

A Spectacular Jet in Comet Hale-Bopp

Astronomers at ESO and elsewhere are now preparing themselves to observe what may become one of the brightest comets of this century.

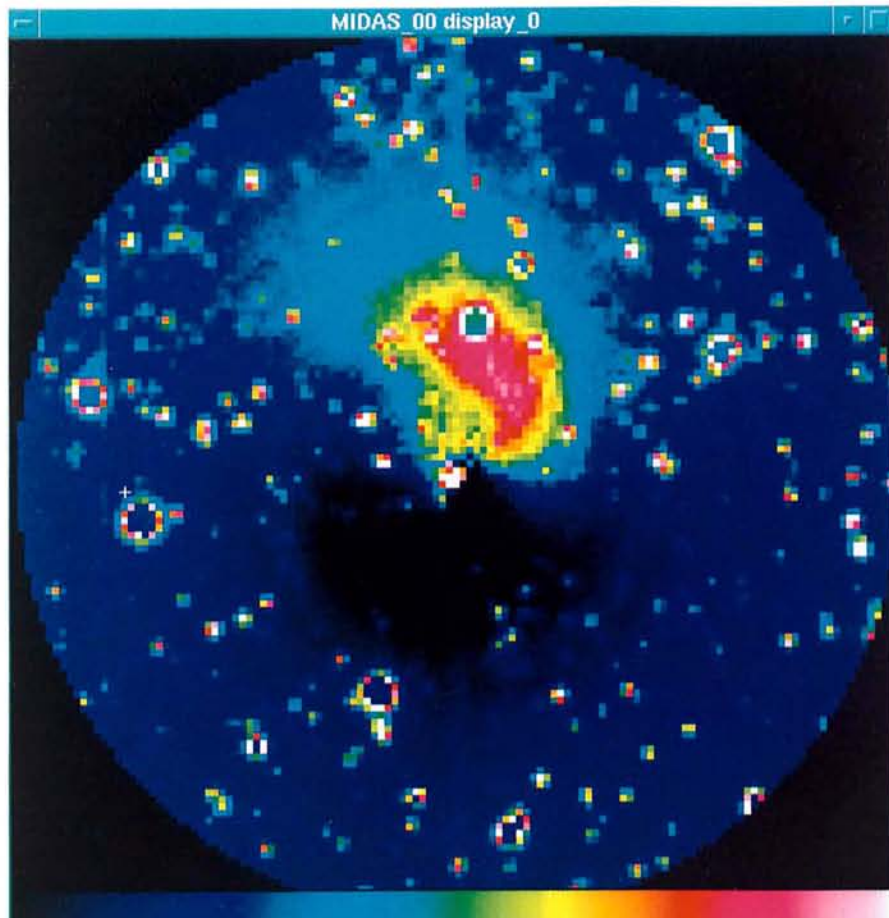
Comet Hale-Bopp was discovered in July 1995, at heliocentric distance 7 AU and already at magnitude 10.5. This is extremely bright for a comet at this large

distance. When it reaches perihelion in early April 1997, and provided the brightness development follows the usual law, it may reach magnitude 0 or brighter. A small ESO Hale-Bopp Task Group has been set up to monitor the further evolution of this very unusual object. Please refer to the ESO WWW Homepage (URL: <http://www.eso.org/comet-hale-bopp/>) for the latest information.

This false-colour image (ESO Press Photo 25/95) shows the large jet now observed in Comet Hale-Bopp. Hans Ulrich Käuffl (ESO) has prepared this computer-enhanced version of a near-IR CCD-frame, obtained on August 31 with the multi-mode DFOSC instrument at the Danish 1.5-m telescope on La Silla by Emilio Molinari from Osservatorio di Brera, Milano-Merate, Italy. North is up and East is to the left; 1 pix = 0.51 arcsec and the circular field has a diameter of 65 arcsec.

The exposure lasted 5 minutes and was made through a Gunn-i filter, recording the reflected sunlight from the dusty coma of the comet at a wavelength of about 9000 Å (900 nm). The observing conditions were excellent (seeing 0.8 arcsec). In order to isolate the light from the jet, the stars were partially removed and the symmetrical part of the coma was subtracted, so that only asymmetrical structures in the frame remain visible.

R. WEST (ESO)



Near-Infrared Imaging of QSO Host Galaxies

J.P.E. GERRITSEN and P.D. BARTHEL, Kapteyn Astronomical Institute, Groningen, The Netherlands

Introduction

Three decades after the discovery of the first QSOs, the triggering of QSO activity is still an intriguing issue¹. Which conditions lead to fuelling the "monster", responsible for the non-thermal continuum emission? The environment may be important, but then: is it the immediately surrounding parsec-scale region, the large-scale intergalactic medium or is it the intermediate galaxy-scale environment (the intergalactic medium) that makes the difference between quiet and active galaxies? Related crucial questions concern the radio-loudness and the nature of the monster: what is the physical reason behind the fact that 5–10% of (UV-excess selected) QSOs develop large extended radio sources, and what is the evidence for black hole mass accretion?

In our project we concentrate on the intergalactic environment for QSOs, but one remark on the cluster environment of QSOs should be made: studies by, e.g., Smith & Heckman (1990) and Ellingson, Yee & Green (1991) indicate that there is a remarkable difference in the cluster environment for radio-loud and radio-quiet QSOs. The former tend to lie in rich clusters while the latter do not. This implies that radio-loudness is a not a phase in the lifetime of an otherwise radio-quiet QSO host galaxy.

As for the host galaxies themselves, they have up till now mostly been studied at the optical wavelengths (e.g., Hutchings, Janson & Neff, 1989, Hutchings & Neff, 1992, Véron-Cetty & Woltjer, 1990). The accepted scenario from these studies is that radio-loud QSOs seem to reside in elliptical galaxies, while most radio-quiet QSOs reside in spiral galaxies. However, some radio-quiet QSO hosts show signs of interaction or signatures of elliptical galaxies. It is clearly an oversimplification to describe these host galaxies as luminous spiral or elliptical galaxies. This is for instance demonstrated by recent HST images (Bahcall, Kirhakos & Schneider, 1994, 1995) and ties in with the idea that QSO activity preferentially occurs in interacting systems (e.g., Stockton 1990).

In the local universe only one type of galaxy can compete with QSOs in total bolometric luminosity: the Ultraluminous IRAS Galaxies. Optical imaging showed that these systems are all in interacting systems (e.g. Sanders et al. 1989). The note that quasar activity may also be related to interactions with companion galaxies has led Sanders et al. to propose an evolutionary connection between Ultraluminous IRAS Galaxies and quasars. In this evolution scenario, merging of gas-rich systems will lead to QSO activity preceded by an ultraluminous far-infrared/starburst phase. Additional motivation for this connection is the comparable local space density for the ultraluminous far-infrared galaxies and QSOs. This scenario suggests that star formation is, or has been, an important ingredient in QSOs.

In several nearby Seyfert galaxies, which can be considered as low-luminosity QSOs, there appears to be a symbiosis of violent star formation and nuclear activity (e.g., NGC 1068, Neff et al., 1994). On intergalactic scales, therefore, one likes to know if there is a relationship between galaxy type and QSO activity and what the connection is between star formation and this activity.

Near-Infrared Observations of Quasar Host Galaxies

The intergalactic environment of quasars can probably best be studied in the Near-Infrared. There the contribution of the active nucleus to the total emission is much lower than in the optical, and so the quasar host galaxies are better seen in the NIR. Moreover, the seeing in the NIR is generally better than in the optical, allowing to detect more structure in the host galaxies. Finally, the optical emission is dominated by emission from massive stars (thus traces recent star formation), whereas the NIR emission is more generated by the old stellar population, i.e. it traces much better the mass of the galaxy.

Recently, imaging in the Near-Infrared has been carried out by two groups: Dunlop et al. (1994) presented K-band observations and McLeod & Rieke (1994) published H-band images. Dunlop et al. conclude from their observations that the

host galaxies for quasars are large galaxies (minor-axis > 40 kpc), while McLeod & Rieke conclude that the host galaxies can be normal L_* spiral galaxies, but not the result of a merger of two L_* spiral galaxies. The galaxies are bluer than normal early-type galaxies (0.5 mag in V–H), indicating there is ongoing star formation in the galaxies or the galaxies have recently undergone a starburst.

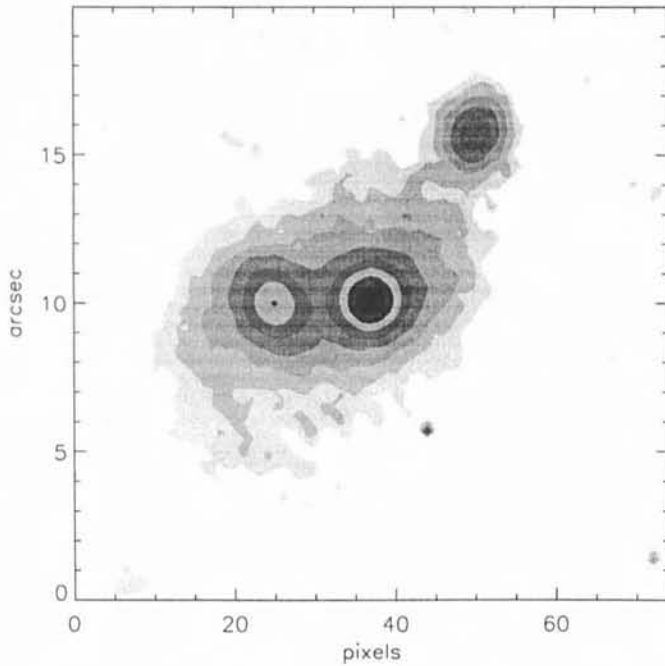
A Near-IR, Radio, and Optical QSO Imaging Survey

In order to investigate the intergalactic structure of QSO host galaxies we are conducting a Near-IR, radio, and optical imaging survey of nearby radio-quiet QSOs. Sample objects were drawn from the Bright Quasar Survey (Schmidt & Green 1983), a UV-excess selected QSO sample. In order to be able to combine the La Silla with the Socorro (NRAO VLA) sky coverage, we selected an equatorial sample, restricting ourselves to $z < 0.36$ objects. Low redshift will enhance chances of observing the host galaxy, enable extracting structure information at sub-kpc resolution, and furthermore allow comparison with ($z < 0.1$) ultraluminous IRAS galaxies. Since the latter are radio-quiet and since radio-quiet QSOs form the majority of the population, we restrict ourselves to radio-quiet QSOs.

The aim of the near-IR images is to get a better knowledge of the QSO host galaxies. Analysis of the J and K colour images will yield information on the structure of the mass component of the hosts. Combined with optical data, the colours of the host galaxies may teach us about recent or ongoing star formation, possibly connected to nuclear activity. To address the question of the importance of star formation in these QSOs further, we will use deep, high-resolution radio data with the sensitive 8 GHz system of the NRAO Very Large Array, at 0.25 arcsec resolution (recall that radio-quiet is NOT radio-silent; typical flux density values for the sample QSOs are 1 mJy). Together with accurate astrometric position measurements of the QSOs (with the aid of the Carlsberg Meridian Circle at La Palma), these data having spatial resolution of order 100 pc will allow us to separate the nuclear and diffuse contribution to the

¹We use QSOs for the combined population of radio-loud and radio-quiet quasi-stellar objects.

PG 1012 J



radio emission and thus the importance of the monster and of circumnuclear star formation to the emission from the quasar. As such, these data will be useful to test predictions of the Warmer model (e.g., Terlevich et al., 1992).

Near-IR Observations and Reduction

The observations were carried out on 2 and 3 March 1995, with the ESO 2.2-metre telescope and the IRAC2B camera. The weather was photometric during one and a half night. Since the objects are small and we are interested in small-scale structure, we used lens B (with a resolution of 0.27 arcsec/pixel) for our observations. The seeing was typically 1 arcsec or slightly better.

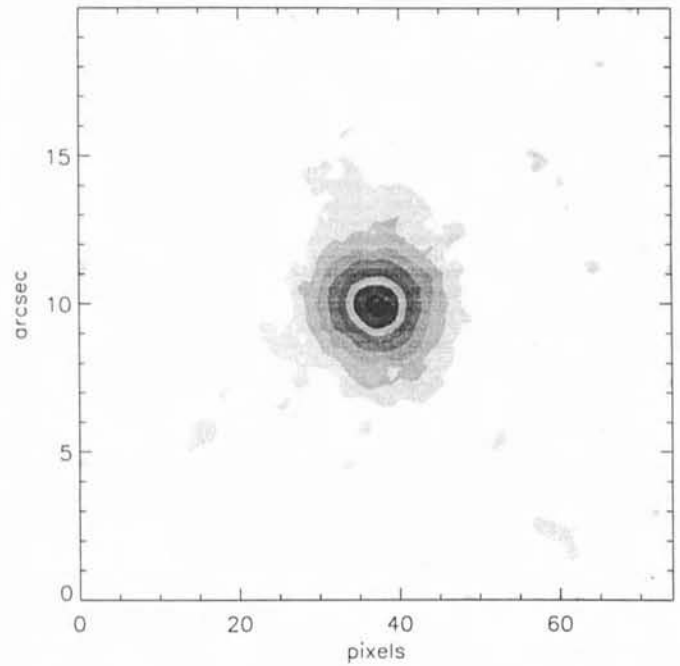
Since all the sample objects are approximately point sources, we could move the objects along the array, thus obtaining object and sky at the same time, without losing observing time by moving to an empty field. In general, we did four integrations of five minutes. In the J window we integrated 20×15 seconds, while we integrated 5×60 seconds with the K filter.

The four images were then median filtered to obtain a local sky frame. From this local sky frame we subtracted a dark frame of the same integration time and normalised it to get a local flat field. We then subtracted the sky frame from individual observations and flat-fielded these to obtain sky-subtracted, flat-fielded images. The four individual frames were added, again using median filtering, to obtain the final image.

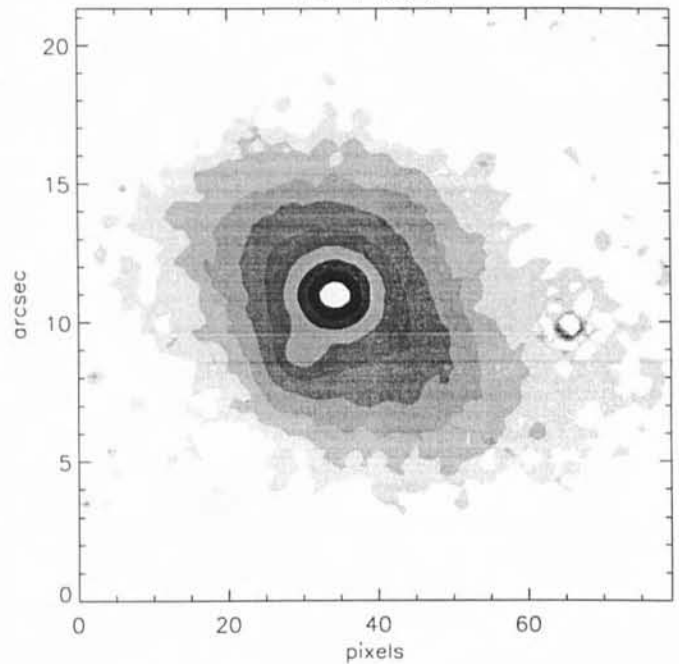
During the nights we regularly observed standard stars for calibration.

J band images of PG 1012+00, PG1049-00, PG 1426+01. Levels increasing in factors of 2, lowest level at 1.5σ ; north to the top, east to the left.

PG 1049 J



PG 1426 J



Since we took only two shifted observations in each filter, we used the science frames for the sky subtraction and dome flat fields for the flat fielding. The photometric accuracy obtained is about 0.1 mag.

First Results

Since we had not yet completed our observing programme while writing this report, the detailed analysis of the data is still in progress. However we can make some general remarks about the host galaxies from the reduced images:

- some quasars are really point-sources,

- other quasars have just faint stuff surrounding the nucleus,

- a few quasars contain multiple nuclei,

- several beautiful galaxies are seen; the largest galaxy (PG1426+01) has a diameter of at least 40 kpc.

It seems that quasar activity may occur in all kinds of galaxies. A next step will be the separation of the nuclear contribution to the images in order to estimate the magnitude of the host galaxies. A comparison of ground-based and HST data shows that the former tend to overestimate the magnitude of the host galaxies, so this task will have to be done very carefully. Interesting will be

HST images in cycle 7 with the NICMOS array.

Some Individual Galaxies

PG 1012+00 ($z = 0.185$, $M_B = -24.33$). This quasar has two secondary nuclei. There is a spiral (or tidal) arm SE of the system. 25% of the radio emission at 5 GHz is diffuse emission, the remainder is slightly resolved at 0.5 arcsec resolution, and has a steep spectral radio index, so may not be nuclear.

PG 1049-00 ($z = 0.357$, $M_B = -25.70$). There is some fuzz extending to the north of the nucleus. The extension is also seen in a R-filter image. At most half of the radio emission at 5 GHz is nuclear, with a flat radio spectrum.

PG 1426+01 ($z=0.086$, $M_B = -23.51$). There is a large asymmetric galaxy under the nucleus and a small secondary nucleus to the SE at 2.5 arcsec (4 kpc) distance. One quarter of the 5 GHz radio emission is diffuse, and the remainder has a steep radio spectrum. As in other sample objects, precise astrometry will tell where exactly the radio emission is located.

References

- J.N. Bahcall, S. Kirhakos & D.P. Schneider, 1994, *ApJL* **435**, 11.
J.N. Bahcall, S. Kirhakos & D.P. Schneider, 1995, *ApJL* **447**, 1.
J.S. Dunlop, G.L. Taylor, D.H. Hughes & E.I. Robson, 1994, *MNRAS* **264**, 936.
E. Ellingson, H.K.C. Yee & R.F. Green, 1991, *ApJ* **371**, 49.

- J.B. Hutchings, T. Janson & S.G. Neff, 1989, *ApJ* **342**, 660.
J.B. Hutchings & S.G. Neff, 1992, *AJ* **104**, 1.
K.K. McLeod & G.H. Rieke, 1994, *ApJ* **420**, 58.
S.G. Neff, M.N. Fanelli, L.J. Roberts, R.W. O'Connell, R. Bohlin, M.S. Roberts, A.M. Smith, T.P. Stecher, 1994, *ApJ* **430**, 545.
D.B. Sanders, B.T. Soifer, J.H. Elias, B.F. Madore, K. Matthews, G. Neugebauer, N.Z. Scoville, 1988, *ApJ* **325**, 74.
M. Schmidt & R.F. Green, 1983, *ApJ* **269**, 352.
E.P. Smith & T.M. Heckman, 1990, *ApJ* **348**, 38.
A. Stockton, 1990, in: R. Wielen (ed.) *Dynamics and Interactions of Galaxies*, Springer-Verlag Berlin, p. 440
M.P. Véron-Cetty & L. Woltjer, 1990, *A&A* **236**, 69.
R. Terlevich, G. Tenorio-Tagle, J. Franco, J. Melnick, 1992, *MNRAS* **255**, 713.

For further information please contact the authors:
gerritse@astro.rug.nl, pdb@astro.rug.nl

Have We Detected the Primeval Galaxies?

D. MACCHETTO¹ and M. GIAVALISCO², Space Telescope Science Institute

The identification of the population of primeval galaxies, namely the first galaxies to form stars in the Universe, is essential to provide the much needed observational underpinning to modern theories of galaxy formation and evolution, without which these theories are destined to remain in the realm of speculation. Until recently, and despite decades of intensive search, primeval galaxies had not been identified and thus the epoch (or the epochs!) and the early physics of galaxy formation are still substantially unknown. The combination of ground-based photometry and spectroscopy with the Hubble Space Telescope high angular resolution, is changing this situation and we are now obtaining empirical evidence that a population of galaxies of relatively normal luminosity was already in place at redshifts $z > 3$ and in an evolutionary state characterised by active star formation.

Thanks to telescopes of large apertures and superior image-quality, and to high-efficiency spectrographs, modern deep-galaxy surveys can now obtain redshift identifications for galaxies at about half the age of the Universe, or redshift of about $z \leq 1.5$. Combined with the morphological information provided by the exceptional angular resolving power of the Hubble Space Telescope, this is providing a reasonably detailed picture of the evolutionary state of the galaxy population over the latter half of the history of the Universe. A consistent result from the work by several groups (Lilly, 1993; Songaila et al., 1994; Glazebrook et al., 1995a and 1995b; Driver et al., 1995a and 1995b; Steidel, Dickinson & Persson, 1994 and 1995) is that galaxy evolution appears to be strongly dependent on luminosity and morphological type. While the population of bright spirals and ellipticals ($L \sim L^*$, with $L^* = 10^{10} L_{\odot}$) have evolved rather passively from redshifts $z \sim 1$ to the present epoch, the fainter galaxies with

luminosity $L \ll L^*$ have undergone a spectacular evolution in morphology, luminosity and number density over the same time span.

The relative lack of evolution in the bright galaxy population suggests that their formation took place at redshifts considerably higher than those probed by the current surveys. Can we observe and track the evolving population of bright galaxies at very high redshifts?

Unfortunately, optical and near-IR spectroscopy of galaxies at redshifts $z > 1.5$ is much harder to obtain due to the limited sensitivity of the current instrumentation and the relative lack of information in the spectral energy distribution which can be probed from the ground. The early primeval galaxy surveys attempted to detect them via their supposedly intense Ly α emission (Partridge and Peebles, 1967; Charlot and Fall, 1993) with optical narrow-band imaging covering the redshift interval $1.8 \leq z \leq 6$. With few exceptions. Noticeably dominated by discoveries made with the ESO 3.6-m and NTT telescopes, including the most distant radio-quiet Ly α galaxy at $z = 3.428$ by Macchetto et al. (1993), no systematic

detections of primeval galaxies have been reported with this technique (see Gialvalisco, Macchetto & Sparks, 1994 for a review). More recently, these surveys have been extended to near-infrared wavelengths to extend the redshift range up to $z \sim 20$ (Thompson et al., 1994 and 1995; Pahre and Djorgovski, 1995) and/or to include emission lines such as [OII] $\lambda 3727$, H β , [OIII] $\lambda\lambda 4969$ 5007, and H α , which do not suffer from the severe attenuation by resonant scattering that affects the Ly α line. With a handful of exceptions, no systematic detections have been reported even in this case. We must conclude that either the redshift ranges searched do not correspond to the epoch during which the presumably violent bursts of star formation took place, or that the theoretical expectations of what a primeval galaxy should look like are not realistic (cf. Baron and White, 1987; Charlot and Fall, 1993).

Recently, a more successful technique to detect primeval galaxy candidates at high redshifts has been pioneered by Steidel and Hamilton (1992). This consists of a redshift-tuned colour photometry derived from broad-band imaging

¹Affiliated with the Space Science Department, ESA.

²Hubble Fellow.

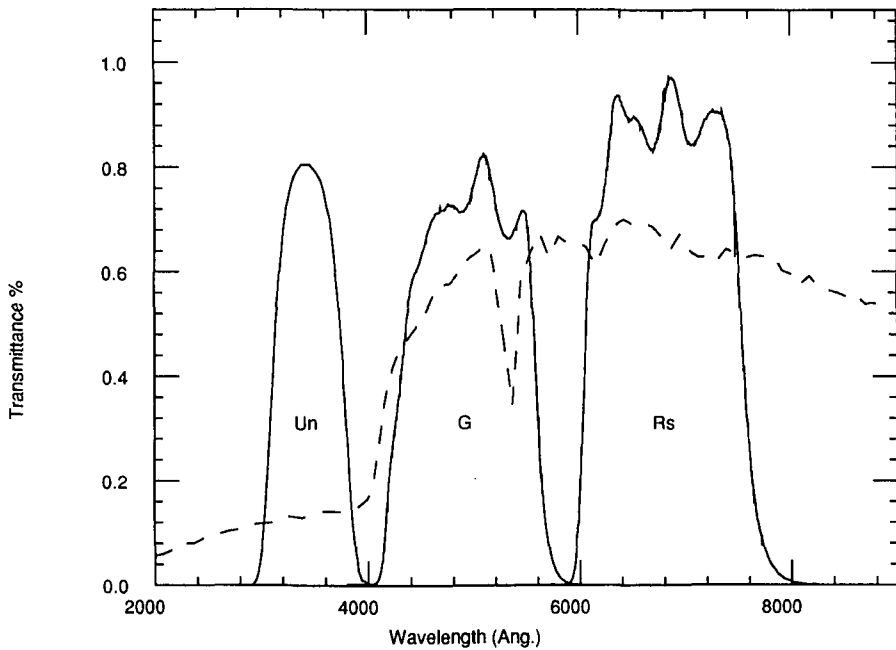


Figure 1: The idea behind the multicolour selection of galaxy candidates at $z > 3$. Shown is the synthetic spectrum of a star-forming galaxy (f_ν units in an arbitrary scale) redshifted to $z = 3.4$ along with the transmission curves of the U_n , G and R passbands. The U_n filter lies entirely blueward of the Lyman discontinuity. The G filter probes the range between the discontinuity and the Ly α line, a region affected by the intervening Ly α forest line-blanketing. Finally, the R filter probes the rest-frame UV continuum redward of the Ly α . Its effective wavelength is intermediate between those of the Johnson R and I passbands so as to provide an improved wavelength baseline, avoiding much of the sky-lines background.

which exploits the presence of the Lyman discontinuity and the Lyman α forest dimming in the otherwise flat and featureless UV spectra of star-forming galaxies. The method takes advantage of the fact that the observable Lyman discontinuity from high-redshift sources, as well as the Ly α forest dimming, is entirely dominated by the intervening QSO absorption systems and is therefore independent of any assumption about the intrinsic discontinuity, which is a function of the initial mass distribution of the forming stellar population (Madau, 1995). It must be stated, however, that any realistic IMF results in a rather pronounced intrinsic Lyman discontinuity, which is made even stronger by the presence of H I.

A customised filter set, i.e. U_nGR , has been designed to provide the maximum colour information and sensitivity (see Fig. 1). The U_n filter is such that the Lyman continuum break is entirely redward of the U_n passband and blueward of the G band, which in turn has a redward upper-limit at the redshifted Ly α wavelength. The R is a compromise between the Johnson R and I bands so as to provide a sufficiently wide wavelength baseline while at the same time avoiding much of the night-sky brightness, and samples the rest-frame UV at about 1600 Å. In practice, star-forming galaxy candidates with redshifts $z > 3$ are selected from colour-colour plots to have very red ($U_n - G$) and moderately blue ($G - R$) colours, respectively. Figure 1 shows the

synthetic spectrum of a star-forming galaxy redshifted to $z = 3.4$ and the transmission curves of the U_nGR photometric system. This technique is sensitive in the redshift range $3 \lesssim z \lesssim 3.5$. The lower limit is dictated by the need to make sure that the Ly α break falls out of the U_n band. The upper limit is set by the amount of Ly α forest absorption, which for higher redshifts becomes so severe that the colours of a high-redshift galaxy become indistinguishable from those of the faint galaxy population (placed at much lower redshifts), even if the filters are modified and tuned to follow the redshifting spectrum. We will refer to the candidates selected with the above method as Lyman-Limit Flat Spectrum (LLFS) galaxies.

Is there any empirical evidence for the existence of a population of forming galaxies with $z > 3$? As a result of the early observations by Steidel and Hamilton (1993), a number of LLFS galaxies have been identified in the field towards Q0000-263 (a quasar with $z_{em} = 4.11$), including the candidate damped Ly α /Lyman-limit system of the QSO at $z_{abs} = 3.389$. These LLFS galaxies have apparent magnitudes consistent with those of

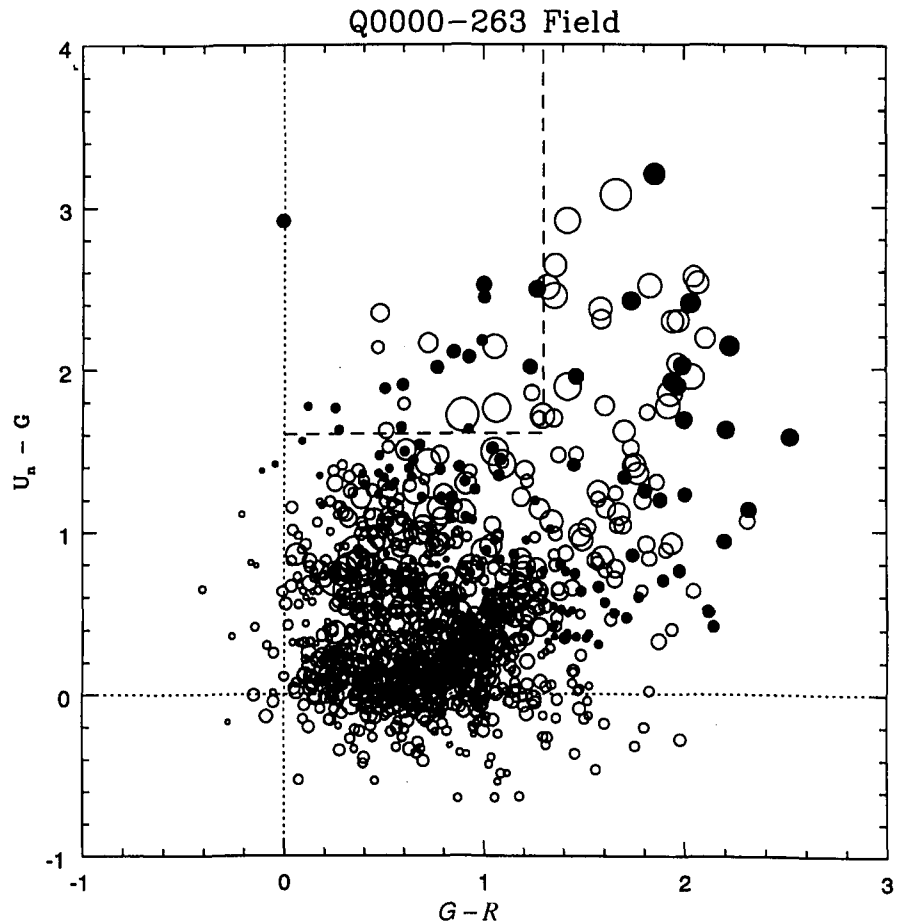


Figure 2: Colour-colour plot $U_n - G$ vs. $G - R$ in AB magnitudes ($AB = -2.5 \log(f_\nu) - 48.595$) obtained with the NTT plus EMMI in the field towards Q0000-263. The vertical and horizontal lines show the locus of flat-spectrum sources, for which the colours are equal to zero in the AB magnitude system. The locus $U_n - G > 1.6$; $G - R < 1.3$ defines the region where to expect galaxies with $z > 3$ (see text). Galaxies in this region have colours rather different from those of the field galaxy population, placed at redshifts $z \ll 3$, with a deviation from the centre of the distribution of $\approx 4\sigma$.

normal bright galaxies, that is with luminosity $L \sim L^*$, caught during a star-forming phase with star formation rates of $\sim 50\text{--}100 h_{50}^{-1} 2 M_{\odot} \text{ yr}^{-1}$ (with $q_0 = 0$), namely $24 < R_{\lambda} < 25.5$ or $2 \leq L/L^* \leq 6$ (assuming an Im spectral type), and are undetected in U_n down to $U_n \sim 27$, with colours $U_n - G > 1.7$ and $G - R < 1.2$. Figure 2 shows a colour-colour plot obtained from our recent NTT U_nGR imaging of the Q0000–263 field (see later). We explicitly note that these colours are *very different* from those of the average field galaxy population. In particular, they show the existence of a *sharp discontinuity* in an otherwise flat (in f_{ν} units) spectral energy distribution, which is not detected in field galaxies.

Madau (1995) has modelled the effects of the stochastic attenuation produced by intervening QSO absorption systems on the broadband colours of cosmologically distant galaxies. His estimates place the identified LLFS galaxies within the realm of what might be called normal, attenuated star-forming galaxies at redshift $3 < z < 3.5$, and show that, if

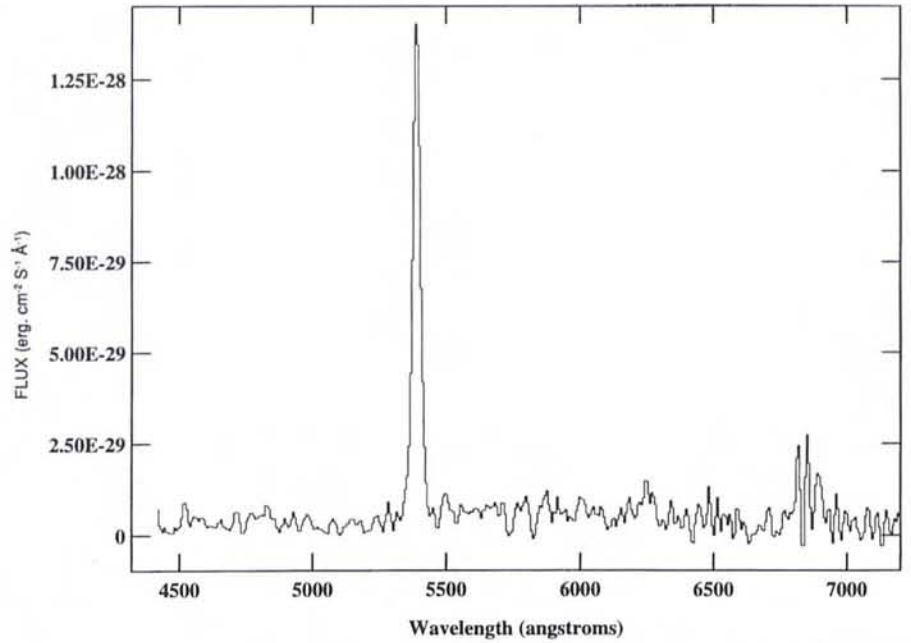


Figure 3: A spectrum of galaxy G2 at $z = 3.428$ obtained with the 3.6-m telescope plus EFOSC1 and PUMA. The total integration time was 8 hours and the resolution is $\sim 19 \text{ \AA}$. Clearly visible is the intense Ly α emission with rest-frame equivalent width of $\sim 170 \text{ \AA}$ and the dimming of the continuum shortward of the line due to the intervening Ly α forest blanketing. No other lines are detected in the spectrum.

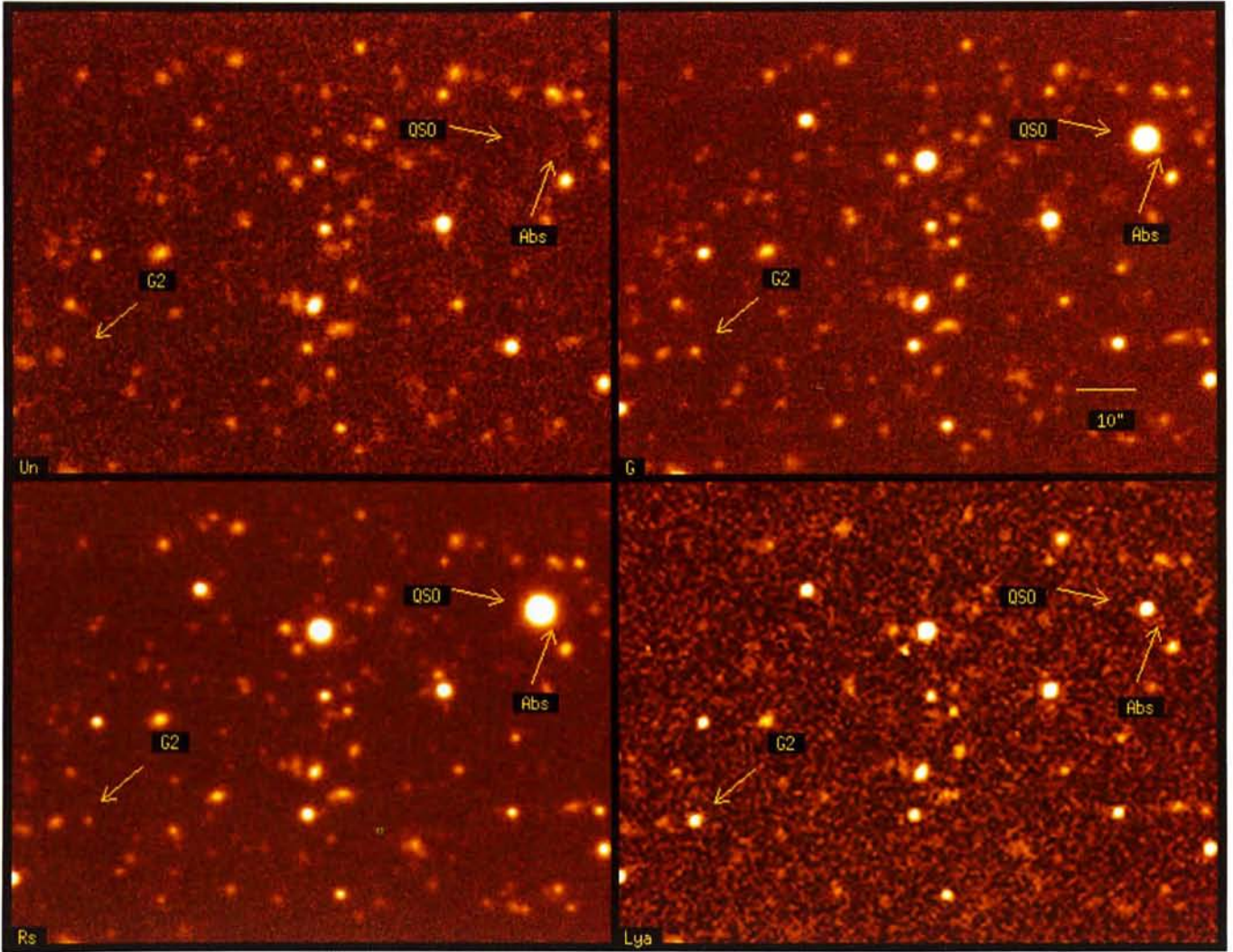


Figure 4: A mosaic showing the U_nGR plus Ly α imaging of the field towards Q0000-262. The four frames show a portion of the field including galaxy G2, the QSO and the absorber (visible in the G frame). The U_n image is from 8 hours exposure with the NTT and EMMI blue. The G and R frames consist of 3 and 2 hours exposure with the NTT and EMMI red. The Ly α frame consists of a 2-hour exposure with the 3.6-m telescope with EFOSC1 and has been obtained with an interferential narrow-band filter (ESO #435). The four frames have been resampled to a common pixel scale of 0.27 arcsec. The seeing of the final stack in each case is about 1.3, 1.1, 1.2 and 1.3 arcsec, respectively.

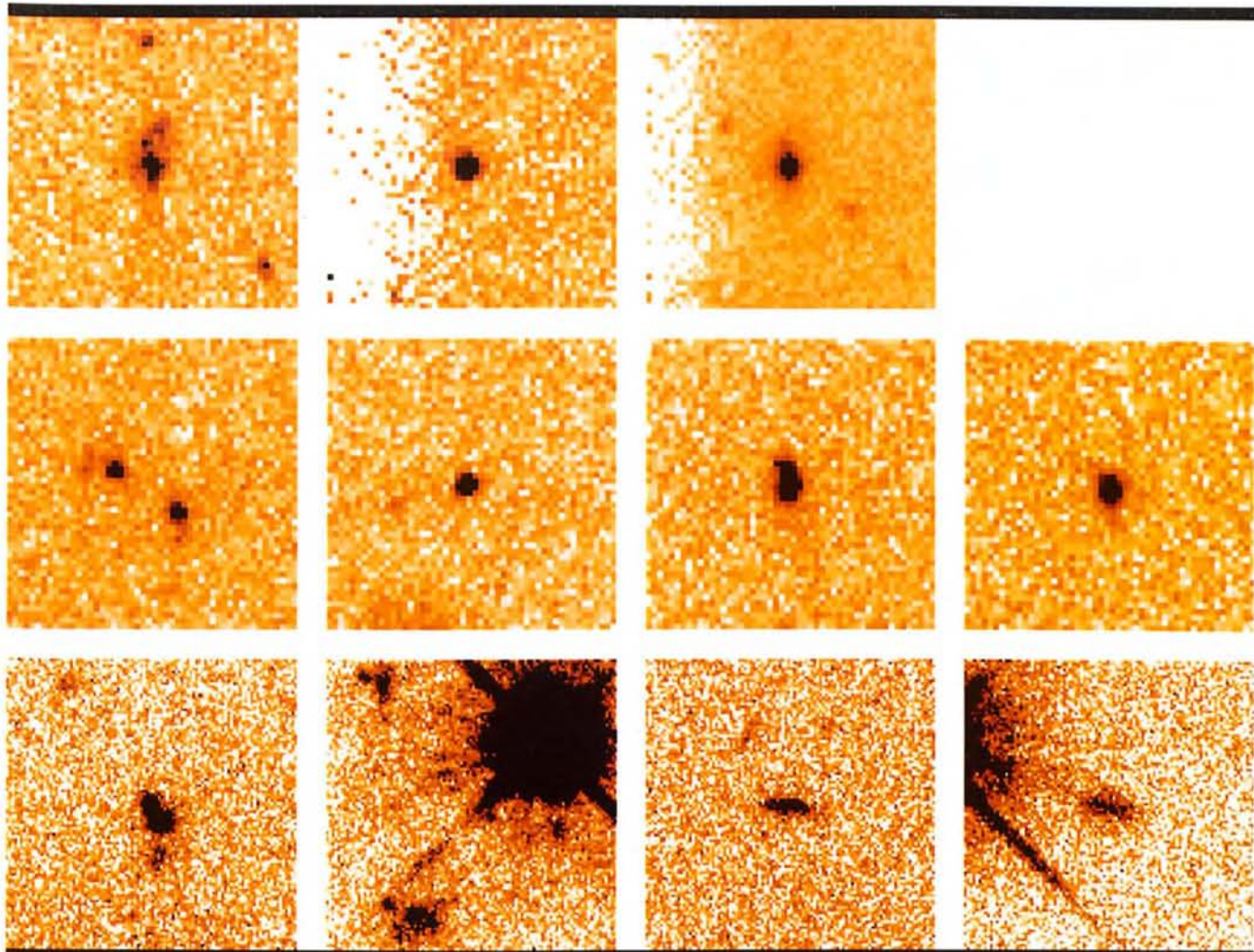


Figure 5: A mosaic of HST images of $z > 3$ galaxy candidates obtained with the WFPC2 camera. The first two rows are from the Wide Field Camera (scale: 0.1 arcsec/pixel). The last row is from the Planetary Camera (scale: 0.046 arcsec/pixel). All images but the two leftmost in the last row are of the candidate members of the $z = 3.4$ putative cluster towards the Q0000-263 field, identified by Giavalisco et al. (1994). They have been obtained with the filter F606W ($\lambda = 5940 \text{ \AA}$) in 4.3 hours of integration. Galaxy G2, the only spectroscopically confirmed candidate so far, is the third from left in the second row. The QSO and the candidate absorber ($z_{\text{abs}} = 3.389$) are in the bottom rightmost panel. The first two images from left in the bottom row are from the field towards Q0347-383, and have been obtained with the filter F702W ($\lambda = 6870 \text{ \AA}$) in 5 hours of integration. The top rightmost image shows a stack of all the WF camera galaxies towards Q0000-263 to show the “average” image of a $z > 3$ galaxy candidate. This image corresponds to 35 hours of integration. Given the large degree of morphological variety that HST imaging has revealed in faint galaxies of comparable apparent magnitude, the strict similarity of the $z > 3$ candidates is surprising and reinforces the idea that we have identified a population of galaxies characterised by common properties. The fact then that their “average” image is so similar to an elliptical galaxy (see also Fig. 6) is very remarkable.

dust extinction is present, it is likely to be small.

In an independent project, using the 3.6-m telescope in combination with EFOSC, Macchetto et al. (1993) and Giavalisco et al. (1994b) have spectroscopically confirmed the redshift of one LLFS galaxy in the Q0000–263 field, a Ly α emitting galaxy at $z = 3.428$ (galaxy G2 in the following), previously found by Macchetto et al. (1993) with a different search technique. This is extremely important, because it empirically demonstrates that among LLFS galaxies there are indeed bright, star-forming galaxies at $z > 3$. Galaxy G2, inconspicuous when observed through broad-band filters longward of U_n ($R_{G2} = 24.2$ or $L_{G2} = 6 L^*$), has a Ly α rest-frame equivalent width of $\approx 170 \text{ \AA}$. We show in Figure 3 a spectrum of the galaxy obtained with the

3.6-m telescope and EFOSC (see also Figure 4, bottom right panel).

Although a quantitative assessment of what fraction of LLFS galaxies are actually star-forming galaxies at high redshift will have to wait for systematic spectroscopic observations (or other equivalent methods, see later), two pieces of evidence already support the fact that we have identified a population of high-redshift star-forming galaxies. The first comes from a clustering analysis of the currently identified LLFS galaxies, while the second comes from the HST observations.

Very interestingly, Giavalisco et al. (1994a) showed that the 14 LLFAS galaxies identified towards Q0000–263 are not homogeneously distributed in the observed field, but are clustered around galaxy G2 and the QSO ab-

sorber. This implies that those 14 galaxies, whose broad-band spectral energy distribution is *identical* to that of G2 and the absorber, are spatially correlated with them, or, in other words, placed at the same redshift. These 16 galaxies are, therefore, members of a “concentration” (a nascent cluster or supercluster?) at $z = 3.4$. This result agrees with the observed strong clustering of Ly α emitters around damped absorbers at very high redshifts (Wolfe, 1993), reinforcing the evidence that clustering characterises the distribution of bright galaxies already at early epochs (incidentally, this suggests that, in general, the fraction of low- or medium-redshift interlopers, which are wrongly classified as LLFS galaxies because of photometric errors, must be small, as there is no reason to expect photometric errors to be spatially

correlated). Thus, we have started to obtain fundamental information that will constrain the theories of structure formation in the Universe, and we have found evidence that an entire *population of galaxies*, was in place and *under construction* at $z \approx 3.4$.

Given the importance of the above results, we decided to obtain even more accurate photometry and search for more candidates in the field towards Q0000–263. We manufactured a set of the U_nGR passbands to match the EMMI specifications (both the blue and the red arm), and we have observed the field for a total of three nights in August 1993. Unfortunately, although the nights were photometric, the seeing was not ideal, ranging from 2.2 to 1.0 arcsec, placing serious limitations on the signal-to-noise. Nevertheless, we have improved the previous observations by about 0.5 mag, obtaining the deepest U_nGR frames so far. We show in Figure 4 a portion of the field observed through the U_nGR filters which include galaxy G2, along with a $Ly\alpha$ image of the galaxy obtained with the 3.6-m telescope. Figure 2 shows the $U_n - G$ vs. $G - R$ colour-colour plot. We will observe the Q0000–263 field again, in the fall 1995, with a set two narrow-band filters designed to probe another sharp discontinuity in the SED of the candidate high-redshift galaxies found, namely the discontinuity around the $Ly\alpha$ wavelength. If these galaxies are really at $z > 3$, the new narrow-band observations, together with the broad-band colours derived from the previous observations, will allow us to constrain the redshifts of the galaxies in a very narrow interval around $z = 3.4$. Thus, although we will not actually measure the redshift with the typical spectroscopic precision, we will nevertheless be able to confirm the nature of our candidates and the existence of a cluster of galaxies at this redshift.

The other very important piece of evidence that supports the identification of the LLFS galaxies with a population of young, bright galaxies at high redshift is their morphological similarity. How do the LLFS galaxies look when observed at the high angular resolving power of the Hubble Space Telescope? WFPC observations by Giavalisco et al. (1995) through the F555W filter have shown that the light profile of the core of G2 is characterised by an $r^{1/4}$ law with $r_0 \approx 1.3$ kpc, with no evidence of an AGN-like central source, while the outer regions exhibit a rather young morphology with elongated structures possibly emitting $Ly\alpha$, and low surface brightness nebulosities. This is suggestive of a relatively recent collapse of the core of G2 which has resulted in a young elliptical galaxy or the bulge of a spiral. Thus, G2 appears to be the progenitor of a bright galaxy,

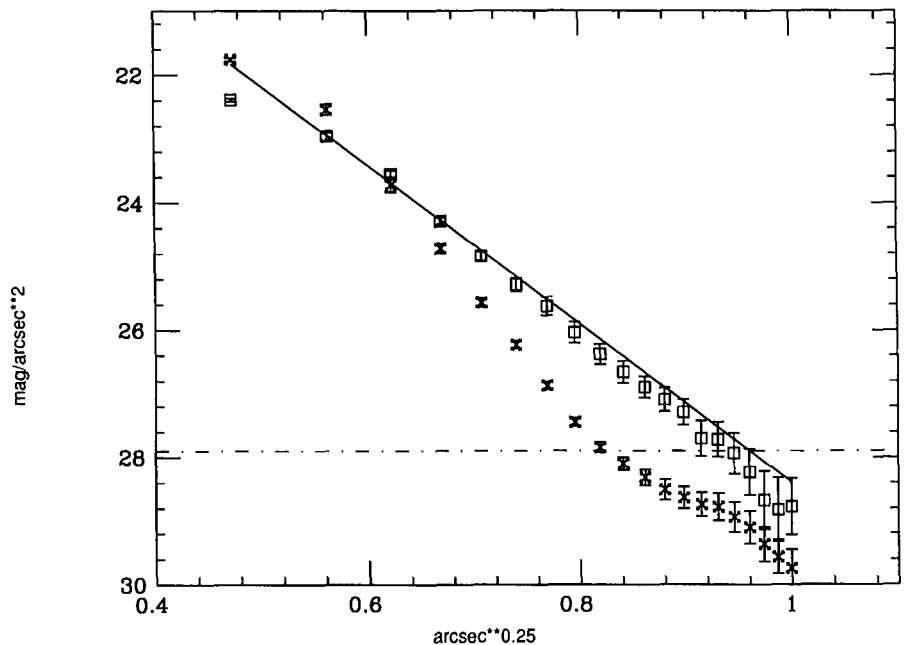


Figure 6: A plot showing the radial light profile of the “average” image of the $z > 3$ galaxy candidates shown in Figure 5, obtained by stacking together 7 galaxies from the Q0000–263 field, including galaxy G2 at $z = 3.428$ (open boxes). The error bars give the 1σ fluctuations along the elliptical isophotes. The crosses show the profile of a star scaled to the same magnitude. The continuous line shows the $r^{1/4}$ law. The dash-dotted line shows the 3σ -level fluctuations of the sky. The data can be modelled by a de-Vaucouleurs law over about 7 mag or 2.8 order of magnitudes.

whose estimated stellar mass at the present epoch would be $M \sim 5^{10-10^{11}} M_{\odot}$, therefore in the observed range of spirals and moderate luminosity ellipticals.

Recent WFPC2 observations by Giavalisco et al. (1995b, in prep.) of the Q0000–263 and other fields have shown a surprising degree of similarity in the morphology of the LLFS galaxies (Giavalisco and Macchetto, 1995, in prep.). These images show that the large majority of the LLFS galaxies are characterised by a compact, or bulge-like, morphology, in some cases surrounded by diffuse, low surface-brightness nebulosities. A minor fraction shows a diffuse, elongated, or disk-like, morphology. Most noticeably, among this subgroup there is the candidate damped $Ly\alpha$ absorber of QSO 0000–263. Wolfe (1986) has proposed that the damped $Ly\alpha$ absorption systems are indeed caused by protogalactic disks, and our observations seem to confirm this view. All the LLFS galaxies have very similar sizes, namely ≈ 1 arcsec in diameter. We show in Figure 5 a mosaic of WFPC2 images of LLFS galaxies from the Q0000–263 and Q0347–383 fields. The upper right panel of the mosaic shows the “average” image of a LLFS galaxy obtained by stacking together all those with compact morphology. Figure 6 shows the light profile of this image obtained fitting elliptical isophotes to it. The continuous line is the $r^{1/4}$ law, which fits the data over more than 2 orders of magnitudes, showing that LLFS galaxies

with compact morphology look, on average, very similar to bulge systems. Given the remarkable variety found with HST in the morphology of galaxies of the same magnitude (but lower redshifts), the extreme similarity of the LLFS galaxies is a rather surprising result, which is now supported on a statistical basis by the relatively high number of these galaxies, observed at high resolution.

In conclusion, our ESO and HST observations have shown the existence of a well-defined class of galaxies, which we have labelled LLFS galaxies. They possess a set of common properties, namely luminosity, spectral energy distribution, and morphology which characterise them as a *true coherent population of galaxies*, and they are currently the *best candidates for the population of primeval galaxies at redshift $z > 3$* . We have spectroscopically confirmed that among these candidates there are objects at redshifts $z > 3$. Furthermore, we have found empirical evidence for the existence of clusters of galaxies at a redshift as high as $z \sim 3.4$. These structures are not predicted to exist at such an early epoch under many theories of galaxy formation. If confirmed by other detections (we are currently working on new fields), these findings will have profound consequences on our understanding of large-scale structure formation and evolution.

With the current sensitivity of the ground-based telescopes, we have access only to the bright end of the luminosity distribution of these galaxies, namely

galaxies with $L > 2-3 L^*$, resulting in very few spectroscopically confirmed detections. Nevertheless, the different pieces of evidence that we have obtained allow us to be very confident in the assertion that we have detected the bright-end of the population of normal galaxies during their early phase of star formation. While we do not yet know whether or not these are the *primeval galaxies*, namely the very first galaxies to form, we are confident that follow-up work with the ESO telescopes and the HST will allow us to build a more meaningful picture for the evolution of galaxies in the early Universe.

References

Baron, E., & White, S. D. M., 1987, *ApJ*, **322**, 585.
 Charlot, S., & Fall, S. M., 1993, *ApJ*, **415**, 580.

Driver, S., Windhorst, R., Ostrander, J., Keel, W., Griffiths, R., & Ratnatunga, K., 1995a, *ApJ*, in press.
 Driver, S., Windhorst, R., Griffiths, R., 1995b, *ApJ*, **453**, in press.
 Giavalisco, M., Steidel, C. C., and Szalay, A. S., 1994a, *ApJ*, **425**, L5.
 Giavalisco, M., Macchetto, F. D., and Sparks, W. S., 1994b, *A&A*, **288**, 103.
 Giavalisco, M., Macchetto, F. D., Madau, P., and Sparks, W. B., 1995, *ApJ*, **441**, L13.
 Glazebrook, K., Ellis, R., Broadhurst, T. J., and Taylor, B., 1995a, *MNRAS*, in press.
 Glazebrook, K., Ellis, R., Santiago, B., and Griffiths, R., 1995b, *MNRAS*, in press.
 Lilly, S. J. 1993, *ApJ*, **411**, 501.
 Macchetto, F. D., Lipari, S., Giavalisco, M., Turnshek, D. A., and Sparks, W. B., 1993, *ApJ*, **404**, 511.
 Madau, P. 1994, *ApJ*, **441**, 18.
 Pahre, M. A., and Djorgovski, S. G., 1995, *ApJ*, in press.
 Partridge, R. B., and Peebles, P. J. E., 1967, *ApJ*, **147**, 868.

Songaila, A., Cowie, L., Hu, E., Gardner, J., 1994, *ApJS*, **94**, 461.
 Steidel, C. C., and Hamilton, D., 1992, *AJ*, **104**, 941, SH92.
 Steidel, C. C., and Hamilton, D., 1993, *AJ*, **105**, 2017, SH93.
 Steidel, C. C., Dickinson, M., and Persson, S. E., 1994, *ApJ*, **437**, L75.
 Steidel, C. C., Dickinson, M., and Persson, S. E., 1995, in preparation.
 Thompson, D. J., Djorgovski, S., and Beckwith, S. V. W., 1994, *AJ*, **107**, 1.
 Thompson, D., Djorgovski, S. G., and Trauger, J. 1995, *AJ*, in press.
 Wolfe, A. M., 1986, *ApJ*.
 Wolfe, A. M., 1993, *ApJ*, **402**, 411.

E-mail address:
 GIAVALISCO@stsci.edu

Discovery of a Supernova (SN 1995K) at a Redshift of 0.478

B. LEIBUNDGUT, J. SPYROMILIO, J. WALSH (ESO); B. P. SCHMIDT (MSSSO); M. M. PHILLIPS, N. B. SUNTZEFF, M. HAMUY, R. A. SCHOMMER, R. AVILÉS¹ (CTIO); R. P. KIRSHNER, A. RIESS, P. CHALLIS, P. GARNAVICH (Center for Astrophysics); C. STUBBS, C. HOGAN (University of Washington); A. DRESSLER (Carnegie Observatories) R. CIARDULLO (Pennsylvania State University)

Three main cosmological parameters govern all models of an expanding Universe. They are the current expansion rate, the Hubble constant H_0 , the derivative of this rate, the deceleration parameter q_0 , and the vacuum energy density, the cosmological constant Λ_0 . Measuring these parameters has been one of the main goals of observational cosmology for the last few decades. As more accurate values of the Hubble constant become available, attention is shifting to the second measurable q_0 which, in a Universe with negligible Λ_0 , is directly linked to the mean density of the Universe (Ω_0).

Reliable distances are needed for a plausible determination of both q_0 and H_0 . While there are now several independent distance indicators which give reliable relative distances out to about the distance of the Coma Cluster, most of these will not work at distances required to measure q_0 primarily due to their limited intrinsic brightness. Type Ia supernovae (SNe Ia) are amongst the more promising distance indicators out to redshifts of about 0.5. SNe Ia exhibit a remarkable uniformity in their light curves and spectra, which, combined with their extremely

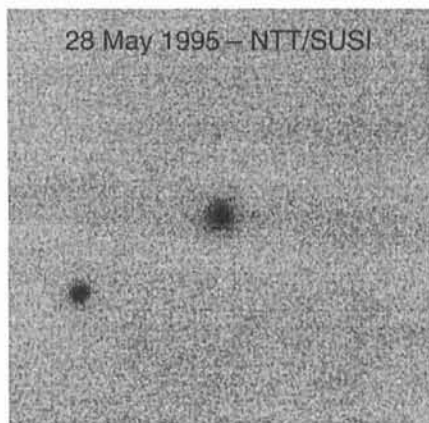
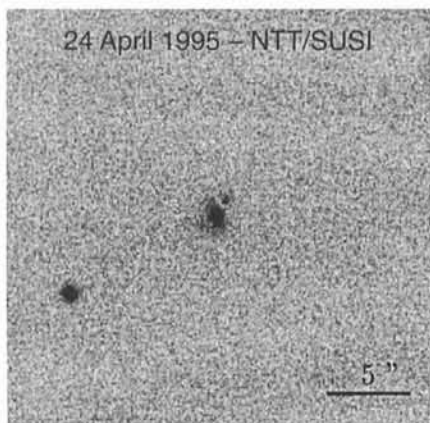
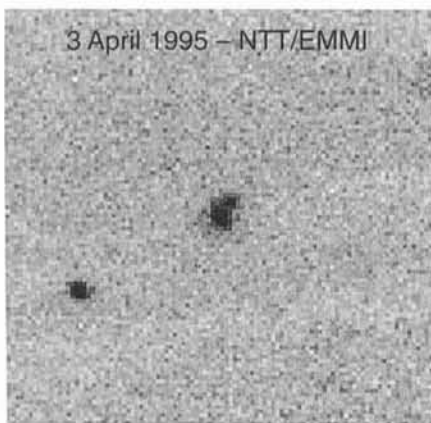
high luminosities make them ideal standard candles. Recent, accurate observations of the SN light curves, however, show that the intrinsic scatter of the absolute magnitude of Ia supernovae exceeds 0.4 magnitudes. This is probably due to variations in the explosion energy and masses of the progenitors. Such a scatter would make supernovae only mediocre standard candles. It has been shown, however, that the absolute magnitude of a SN Ia is correlated with its light curve shape. This makes it possible to correct supernova magnitudes as long as a well-observed light curve is available. A sample of SNe Ia with redshifts of less than 0.1 follows the expansion relation in the z vs. m_{max} diagram extremely well and, after the aforementioned correction is applied, with a very small scatter (< 0.2 mag; Hamuy et al., 1995).

We have started a project to search for supernovae at redshifts between $0.3 < z < 0.5$ combining several 4-m-class telescopes around the world. The search is conducted with the CTIO 4-m prime focus camera which provides a field of view of 15 arcmin on a side. Short exposures (5 minutes) reach a limiting magnitude of about 23.5 in a special redshifted B filter (almost equivalent to a

regular Kron-Cousin R filter). We can observe around 55 fields in one night. Specially designed search software is employed in real time to find suitable candidate objects by comparing the newly acquired frames with reference images obtained on previous runs. Spectroscopic follow up time has been scheduled at the AAT, the MMT, and the NTT at ESO. These nights have been requested to follow shortly after the search nights making it possible to obtain a spectrum of any supernova discovered near maximum. We expect to find most supernovae slightly before peak light due to special spacing of the search nights.

Reference images of the fields were established last February followed by three search nights in February and March. Unfortunately, the weather was clear only during two half nights in March. A good candidate was established during our last search night at CTIO and was followed up two nights later with the NTT. The possibility to use the various modes of EMMI and the high spatial resolution of SUSI during a single observing night allowed us to confirm the existence of the supernova, now designated SN 1995K (Schmidt et al., 1995), in a distant galaxy

¹now at ESO.



A sequence of images of SN 1995K taken with the NTT. The first image (left) shows the supernova near maximum light. Three weeks later the object has faded considerably (middle) and is not detected two months after discovery. The stretch of the images is comparable to show the brightness decline of the supernova. The seeing measured from stars in the images was 0.8, 0.5 and 0.7 arcseconds from left to right.

and to obtain a spectrum of both the supernova and its galaxy.

The galaxy spectrum shows emission lines of $H\alpha$, [N II], weak [O III], and $H\beta$ lines corresponding to a Sbc galaxy spectrum at a redshift of 0.478. An additional spectrum obtained at CTIO one month later confirms this conclusion.

An essential ingredient for the use of a high-redshift supernova as a distance indicator is its classification. The current classification scheme of supernovae is based on spectra around the maximum brightness of the event. For a meaningful and secure distance determination it is of paramount importance to classify the supernova by obtaining a spectrum. Since a supernova at a redshift of 0.4 reaches a peak brightness of $m_R = 22.3-23.3$ (depending on q_0) this is not a simple task.

The spectrum of SN 1995K is heavily contaminated by the galaxy (the supernova is located only 1.1 arcseconds from the galaxy nucleus). Nevertheless, it appears consistent with a regular SN Ia at maximum. The defining absorption line of [Si II] near 6100 Å can be seen near 9000 Å in our spectrum, a region severely affected by night sky lines.

Preliminary photometry indicates a peak magnitude of about 22.7 in R which explains some of the difficulties in obtaining a decent spectrum. The light curve of SN 1995K has been estab-

lished through observations at the NTT, the 3.6-m and the Danish 1.5-m at ESO, and the 2.5-m DuPont telescope on Las Campanas. Whenever possible, we observed SN 1995K through special filters which correspond to B and V filters redshifted to 0.45. This technique makes uncertainties due to K-corrections (due to the redshifts) minimal. Since the regular R filter is almost identical to B redshifted to 0.47, we have included observations using this filter as well. The decline rate should be easily measurable from our photometry, and the possibility to measure a reliable distance is promising. Only modern image-processing techniques allow us to extract accurate magnitudes from an object which is deeply embedded in its host galaxy like SN 1995K. The available SUSI images (see Figure) obtained under very good seeing conditions will play an important role as templates for the extraction of the supernova magnitudes.

SN 1995K is the most distant star observed to date. It is among the half dozen supernovae at $z > 0.3$ known so far (Nørgaard-Nielsen et al., 1989, Perlmutter et al., 1994, 1995). The discovery of this supernova is proof that our programme is working. We were predicting one or two supernovae for our trial period. The next step is the establishment of reference images for the second half of

the year (October/November) with the CTIO telescope and a continuation of the search early next year. With an improved version of the search software and several lessons learned from the pilot project we are well-prepared for more distant supernovae to be discovered.

For a reliable measurement of q_0 we will need more supernovae. We estimate that about 20 supernovae with accurate peak magnitudes are needed to put significant constraints on the deceleration of the Universe. Combining our results with similar projects under way at the Lawrence Berkeley Laboratory we should be able to reach this goal in the next few years. One of the main obstacles right now is the availability of good spectroscopic data. More photons would greatly enhance our ability to take spectra of these objects.

References

- Hamuy, M., et al., 1995, *AJ*, **109**, 1.
 Nørgaard-Nielsen, H. U., Hansen, L., Jørgensen, H. E., Salamanca, A. A., Ellis, R. S., and Couch, W. J., 1989, *Nature*, **339**, 523.
 Perlmutter, S., et al., 1995, *ApJ*, **440**, L41.
 Perlmutter, S., et al., 1994, *IAU Circ.* 5956.
 Schmidt, B. P., et al., 1995, *IAU Circ.* 6160.

E-mail address:
 B. Leibundgut, bleibund@eso.org

The Magellanic Catalogue of Stars – MACS

K.S. de BOER¹, H.-J. TUCHOLKE^{2,1}, and W.C. SEITTER²

¹Sternwarte der Universität Bonn; ²Astronomisches Institut der Universität Münster

Introduction

The Magellanic Clouds harbour a vast number of objects of interest for the observer. In many cases it is, however,

difficult to find accurate coordinates for stars in crowded fields of the Clouds. A first step to solve this problem was made by Périé et al. (1991), who published a catalogue of almost 1000 stars in the

direction of the Magellanic Clouds with typical V magnitudes between 9 and 11. The positions are based on ESO Schmidt plates and have a positional accuracy of 0.5". This catalogue can be used as

reference catalogue to obtain star positions on, e.g., astrographic plates.

In order to have enough reference stars for CCDs, however, a much higher surface density of stars is needed. De Boer (1993) presented plans for such a catalogue. The first version of it is now available. The **Magellanic Catalogue of Stars (MACS)** is based on scans of ESO Schmidt plates and contains about 244,000 stars covering large areas around the LMC and the SMC. The limiting magnitude is $B \leq 16^m.5$ and the positional accuracy is better than $0.3''$ for 99% of the stars. The stars of this catalogue were screened interactively to ascertain that they are undisturbed by close neighbours.

Plate Material, Measurement, and Selection

The MACS is based on plates taken with the ESO Schmidt telescope between November 1988 and January 1989 (a few plates taken in 1991 were also used). The exposure time was 60 minutes in the blue passband Ila-O + GG 385. The limiting magnitude is $B \approx 20^m.5$. The plate centres are the same as in the ESO/SRC survey. The plates were intended as a repetition of the ESO Quick Blue Survey with the aim of deriving absolute proper motions of the LMC and the SMC, measured with respect to background galaxies (Tucholke and Hiesgen, 1991). We used 21 plates of 12 fields, so that most fields were covered by two plates. The MACS in its present version covers an area of about 200 and 120 square degrees for the LMC and the SMC, respectively (Figs. 1a, b).

The Schmidt plates were digitized with the PDS2020 GM^{plus} microdensitometers of the Astronomical Institute of Münster University. A fully automatic programme (Horstmann, 1992) was used for the detection of objects. For the MACS, the parameters of this programme were chosen to yield a limiting magnitude of about $B = 16^m.3$. This limit was checked using CCD photometry from the literature. Since published photometry is not available for all fields, we had to rely on the homogeneity of the plate material. From comparison of the internal magnitudes in plate overlap regions we found that the limiting magnitudes scatter by $\pm 0^m.2$.

A very time-consuming step is the *interactive screening* of all detected objects. The aim of the selection is to provide the catalogue user with reference stars which are apparently *undisturbed* by neighbouring stars on the Schmidt plates. We excluded stars having close neighbours with separations of about $2''$ to $11''$. Galaxies and artifacts were removed from the data base during this viewing. The efficiency of the screening against double stars varied somewhat with crowding conditions: in very crowded

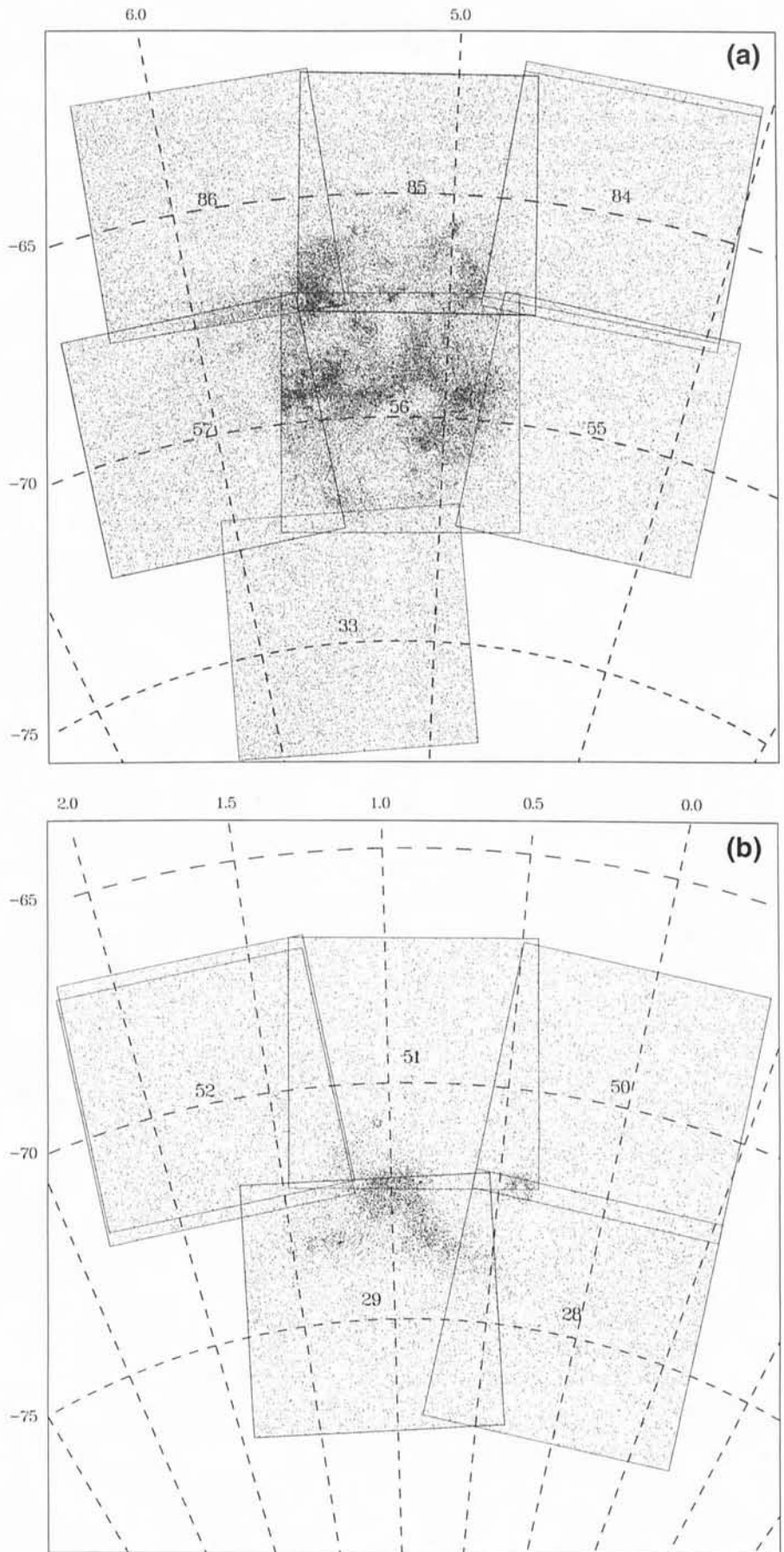


Figure 1: (a) Sky distribution of 175,779 MACS catalogue stars towards the LMC. Also given are numbers identifying the ESO/SERC atlas fields, the outlines of the plates used, and a J2000.0 co-ordinate grid. The largest concentrations of catalogue stars are found near active star-forming regions, while the bar contributes relatively few stars brighter than $B = 16^m.3$. (b) 67,782 catalogue stars in the direction of the SMC. The outer wing is not yet included in the catalogue. Note the concentrations around the galactic globular clusters 47 Tuc and NGC 362.

fields small perturbations were tolerated in order to keep a sufficient number of stars. Note that discarded stars might be undisturbed by their neighbours on CCD frames due to a more favourable scale. What matters here, however, is reliable photographic reference positions. The screening is a major improvement relative to catalogues compiled in a non-interactive way like the Guide Star Catalog or the ROE/NRL Catalogue. The second author inspected $\approx 529,000$ objects selected by the search programme, 422,000 of which passed this procedure.

Astrometry and Positional Accuracy

The computation of right ascensions and declinations (α , δ) from the plate coordinates used between 160 and 220 reference stars fainter than 9^m0 from the PPM South Catalogue (Bastian et al., 1991). Positions from Schmidt plates, obtained by transforming plate to celestial coordinates using low-order polynomials, frequently show systematic patterns when compared to independent catalogues (Taff et al., 1990). This effect is probably caused by the bending of the plates to the curved focal plane during exposure. Our case is no exception. Since all plates were exposed, developed and scanned in a similar way, we combined the residuals from all 21 plates into a two-dimensional array as a function of x and y . We found a clear systematic pattern (Tucholke et al., 1995) and subtracted it from the measured (x , y)-co-ordinates. This reduces the mean residuals to 0.18" in both co-ordinates. Although individual plates do not strictly adhere to this systematic pattern, an individual correction for each plate is not feasible, since the number of PPM stars per plate is still too low to allow a sufficient spatial resolution.

A first check on the accuracy of the MACS is provided by the comparison of the two plates available for most of the fields. Comparison of (α , δ) yields an r.m.s. scatter between 0.12" and 0.19" per co-ordinate. Typical amplitudes of systematic differences are 1–3 μ m, corresponding to 0.07" . . . 0.20". Internal magnitudes agree within 0^m11 . . . 0^m19 after correction for the different limiting magnitudes.

The regions of overlap between neighbouring plates (see Figs. 1) yield an extreme test of the positional accuracy. R.m.s. differences are 0.34" . . . 0.42"; thus the accuracy on one plate is 0.24" . . . 0.30". The scatter of the internal magnitudes about the mean difference ranges from 0^m12 to 0^m18.

The Catalogue

In the present version, the MACS contains data for 175,779 and 67,782

TABLE 1. SOME LINES FROM THE PRELIMINARY MACS FOR STARS IN THE FIELDS OF NGC 330 (SMC) AND SN 1987A (LMC).

Name	α_{2000}	δ_{2000}	N	Mag.	Flags		
					Pos	Mag	Bochum
⋮	⋮	⋮	⋮	⋮	⋮	⋮	⋮
MACS J0056–724#003	0 56 03.321	–72 29 07.80	1	16.56	0	0	0
MACS J0056–724#005	0 56 06.837	–72 28 35.25	1	17.81	0	0	0
MACS J0056–724#006	0 56 07.449	–72 29 28.38	2	18.19	0	0	0
MACS J0056–725#005	0 56 13.847	–72 30 00.32	2	17.49	0	0	0
MACS J0056–724#010	0 56 24.076	–72 29 14.48	2	17.04	0	0	0
⋮	⋮	⋮	⋮	⋮	⋮	⋮	⋮
MACS J0535–692#022	5 35 30.401	–69 16 18.13	1	19.33	0	0	0
MACS J0535–692#024	5 35 32.625	–69 15 48.53	4	19.14	0	0	0
MACS J0535–692#025	5 35 34.493	–69 17 13.58	1	99.00	0	1	0
MACS J0535–693#024	5 35 34.828	–69 19 19.53	1	19.98	0	0	0
MACS J0535–692#027	5 35 36.136	–69 16 08.96	4	17.98	0	0	0
⋮	⋮	⋮	⋮	⋮	⋮	⋮	⋮

Note: The name of the object consists of the acronym MACS (for Magellanic Catalogue of Stars, but one can also read it as Magellanic Cloud Star), the letter J denoting the equinox J2000.0 to which the position refers, a position code for the upper right (NW) corner of the box with size 1^m × 6', and the #nnn giving the running number of the star inside that box. This format is in agreement with the Rules and Regulations for Nomenclature as defined by IAU Commission 5.

stars in the direction of the LMC and SMC, respectively. The surface density of stars in non-crowded regions is 0.15 stars/□'. This is just sufficient to yield for a modern CCD covering 25□' on the average the minimum number of 4 reference stars.

A name was assigned to each star following the suggestion of de Boer (1993), giving its truncated position and a running number within an (α , δ)-box of 1^m × 6'. This format allows to add further stars inside the box to the catalogue without upsetting the numbering system. Table 1 shows the data for some stars in the vicinity of SN 1987A (LMC) and the young globular cluster NGC 330 (SMC).

The star positions are given for the equinox J2000.0 and the epoch 1991.0, compiled from up to 8 plates. As a typical accuracy (within the PPM system) we take 0.27" from the r.m.s. scatter in the overlap regions. Less than 1% of the stars carry a flag that the internal positional error is larger than 0.5". Instrumental magnitudes are given in a blue passband. They are corrected to a common, arbitrary zero point for the LMC and the SMC, respectively, and should be useful at least for identification. Just 0.6% of the stars had to be flagged as having an above-average plate-to-plate scatter of internal magnitudes, either from bad photometry or due to variability.

Proper motions could not be derived, since the plates were taken at more or less the same epoch. This limits the usefulness of the catalogue as an astrometric reference. However, in crowded fields one can hope that the majority of stars are MC members with a common proper motion, thereby minimising this problem. In the future, we plan to add proper motions to our catalogue (a few plates from the ESO Quick Blue Survey have already been scanned).

First attempts in using the MACS as a reference catalogue for CCDs in very crowded fields revealed large difficulties in the identification process, since for our catalogue many stars had been discarded due to disturbing neighbours. This problem can be alleviated by distributing a zoomed-down version of the original scans, with the catalogue stars marked.

The MACS has up to now been cross-identified only with the catalogue of Périé et al. (1991), showing r.m.s. differences as expected from the internal errors. An identification with the Guide Star Catalog will follow. An important cross-identification, to be done before the first official release, will relate the MACS to the data base currently being compiled at the Astronomisches Institut Bochum containing astrophysical information on thousands of (relatively bright) stars in the direction of the LMC.

A detailed description of the creation and content of the MACS will be given in a forthcoming paper (Tucholke et al., 1995). Colleagues interested in a preliminary version of the catalogue should contact us under the e-mail address tucholke@astro.uni-bonn.de.

References

- Bastian U., Röser S., Nesterov V.V., Polozhentsev D.D., Potter Kh.I., Wielen R., Yagudin L.I., Yatskiv Ya.S., 1991, *A&AS* **87**, 159.
- de Boer K.S., 1993, in "Recent Advances in Magellanic Cloud Research", eds. Baschek B., Klare G., Lequeux J., Heidelberg: Springer, p. 389.
- Horstmann H., 1992, Ph.D. Thesis, Astron. Inst. Univ. Münster (in German).
- Périé J., Prévot L., Rousseau M., Peyrin Y., Robin A., 1991, *A&AS* **90**, 1.
- Taff L.G., Lattanzi M.G., Bucciarelli B., 1990, *ApJ* **358**, 359.
- Tucholke H.-J., Hiesgen M., 1991, IAU Symposium No. 148, 491.
- Tucholke H.-J., de Boer K.S., Seitter W.C., 1995, *A&AS*, in preparation.

Remote Observing and Experience at ESO¹

A.A. ZIJLSTRA, J. RODRIGUEZ AND A. WALLANDER, ESO

1. History

Remote observing has been widely used in radio astronomy for the last decade. However, in the optical and infrared domain very few observatories have been successful in supporting it. One reason for this difference is that optical/infrared telescopes are more demanding in the sense of object acquisition and amount of science data produced. Another reason could be that optical astronomers have less trust in the performance of the telescope and instruments.

In the early 1980's a number of observatories started experimenting in remote observing (Raffi and Tarengi, 1984, Longair et al., 1986, Raffi and Ziebell, 1986). Most of these early attempts failed, mainly because the technology was not yet matured. The communication links were not reliable and the data transmission rates were too low. It also became evident that it was very difficult to operate a telescope originally designed for local control in remote mode.

In the late eighties the situation became more favourable. First, there was a general improvement in communication infrastructure: cheaper, more reliable and faster, not to forget the development of Internet and, more recently, of the World-Wide Web. Second, a new generation of 3–4-m class telescopes were designed and went into operation. For some of these, remote observing had been foreseen already during the design phase (Loewenstein and York, 1986, Raffi et al., 1990).

Remote observing comes in many different modes, starting (or ending) at fully automatic telescopes. In 1992 a workshop dedicated to remote observing was held in Tucson (eds. Emerson and Clowes, 1993), where many of the available forms were extensively discussed. We will first summarise the terminology adopted at this conference for the various remote-observing modes, before describing the present situation at ESO.

2. Definitions

- *Robotic Telescopes* – A telescope and instrument which is programmed beforehand and needs little or no attention during the night. An entire nights observing programme may be downloaded during the day and the scientific data uploaded during the observation or later.

- *Remote Engineering* – A remote engineer performs engineering activities, e.g. installations, diagnostics, troubleshooting, on local equipment. Although this is not an observing mode it should be included in the context, because if remote engineering is available, remote observing may come for free. Remote engineering can be very effective, especially since often engineers need to come to the telescope for relatively minor tasks and the travel distance can be significant.

- *Service Observing* – An astronomer fully specifies the objects to be observed and the instrument configuration beforehand, and the actual observation is carried out by the observatory staff. The astronomer is awarded observational data rather than telescope time.

- *Passive Remote Observing* – A remote observer monitors an observation carried out at a telescope by a collaborator or service observer. The remote observer has access to the data obtained and, optionally, observation parameters, and interacts with the local observer via voice, "talk", or e-mail. This is also called Eavesdropping. It is probably fairly common for the larger telescopes but observatories tend not to keep track of this.

- *Active Remote Observing* – A remote observer interactively controls an instrument and, optionally, a telescope at an observatory. In most cases a local telescope operator is required for safety reasons and sometimes to operate some

telescope and auxiliary equipment. This is also called *Remote Control*.

Combinations of these observing modes are of course possible, and may in fact give additional advantages.

Robotic telescopes are by far the most popular of these options. They are typically small telescopes (50 cm). There are two important uses: the first is for long-term monitoring programmes (an example is the network of small telescopes looking for solar oscillations) and the second is for educational purposes. Some universities now have a small robotic telescope where astronomy students can send in requests electronically for short observations: this is especially useful for astronomy classes with many students in poor astronomical sites. One could also see automatic seeing monitors or small telescopes for measuring extinction coefficients as robotic telescopes.

At the other extreme, *active remote observing* is rare. The only large telescope for which this mode is the norm is the 3.5-m on Apache Point Observatory (APO), which is run by a consortium of US universities. This telescope is operated for 80% of the time available for scientific observations in remote control. Typically, a night will be split between several projects, and each astronomer can carry out the observations from his or her campus. ESO has two telescopes which can be operated in remote control: the 1.4-m CAT which is used for high-resolution spectroscopy mainly of bright stars, and the 3.5-m NTT.

3. Pros and Cons

The motivation for remote observing has been debated for some time in the literature, and a high level of agreement on the main arguments has been ob-

TABLE 1. WEIGHING THE PROS AND CONS OF REMOTE OBSERVING.

Proven Advantages	Likely Advantages	Likely Disadvantages	Proven Disadvantages
Flexibility	More than one participating astronomer	More difficult to concentrate on observing	Expensive - personnel - comms.
Shorter observing programs	May save costs in some cases	Not as efficient as classical	
Convenient for astronomer			

¹This article is an edited version of a paper submitted to the Astronomical Society of the Pacific (ASP) for publication in the ASP Conference Series. Copyright Astronomical Society of the Pacific, 390 Ashton Avenue, San Francisco, California 94112.

tained (e.g. Emerson and Clowes, 1993). These arguments are summarised in Table 1 and briefly discussed below.

The main arguments in favour of remote observing are all related to the fact that the astronomer does not need to travel to the observatory. This is a strong argument if the observatory is in an inaccessible place, the most extreme example being the planned observatory on the Antarctic Plateau for which remote observing is envisaged (Burton, 1995). It also allows for the observing schedule to be made at short notice (e.g. the VLA). However, flexible and queue scheduling is not recommended in active remote control and/or eavesdropping: for the astronomer to be directly involved, the time of the observations needs to be known in advance. Instead it is possible to schedule shorter observing programmes, in units of hours instead of nights. Monitoring programmes also become easier to schedule without an astronomer at the observatory having to be involved. The elimination of long travel times and acclimatisation results in savings of astronomer's time – an important point for researchers at universities who may have teaching duties.

Remote observing very often allows more than one astronomer to take part in the observations. The impression at ESO is that, for the large telescopes, astronomers prefer to come with more than one person: while one person does the observing, the other concentrates on the on-line data analysis. For remote control, financial support for an extra observer is easier to arrange. The experience at ESO (NTT) is that in almost all cases, the home institute pays for a second observer in addition to the one paid for by ESO, in the case of remote control. This may increase the efficiency of the observations, but may also be of importance from an educational point of view. In addition, for the 1.4-m CAT telescope we also attract some Eastern European astronomers who could possibly not afford to travel to Chile. For them remote observing can save costs, but for the observatory this will in general not be true unless the required communication links are free, or very cheap, and little additional support is required.

Cost is the main argument against remote observing. In order not to degrade the scientific efficiency, the remote observer must get the same support as the local observer. This means that often the support personnel have to be duplicated. Sufficient bandwidth is also required in order not to have idle telescope time, and the cost of this bandwidth can very easily overtake the savings in travel cost. Table 2 shows typical cost estimates for the case of ESO², showing that remote observing only reduces total costs when it is used for a significant fraction of the observing proposals for at least two telescopes. A second argument against remote observing is, that, due to limitations in bandwidth, there is a time delay before the observer sees the data coming from the instrument. (This problem is not unique to remote observing but is experienced by everyone observing with CCDs.) The experience at ESO is that this becomes a problem whenever the extra delay is a significant fraction of the average integration time per exposure. Finally, if the observations are done from one's own office, the distractions due to the normal office activity may easily cause a loss of efficiency.

4. Requirements and Techniques

The main requirement for all modes of remote observing is a fast data transfer from the observatory to the remote site. Data files produced by modern instruments are large (a typical CCD frame is 2 to 8 Mbytes), and they should ideally be transferred in no more than a few minutes. To achieve this, a fairly high bandwidth is required, although modern data compression algorithms can improve the transfer rate. Compression based on the H-wavelet transform have been successfully applied at a number of observatories. In comparison, the data

²Assumptions:
Classical observing run (travel, accommodation, etc.) = kDM 4
Remote observing run (travel, accommodation, etc.) = kDM 0.8
Remote operator = kDM 10/month
Link cost (50%) = kDM 18/month
Same local support for classical and remote observing.

rates required to operate the telescope are tiny. However, for active remote observing, no delays in transmitting the requests can be tolerated. Both the availability and the reliability of the communication link need to be very high.

A second requirement is that the telescope and instrument must be reliable and stable. Solving technical problems is more difficult during remote observing. A good way to limit unforeseen problems is by keeping instrument change-overs to a minimum. Limiting the instrumentation is also a better way to ensure adequate know-how at the remote-observing site.

Internet is certainly the main carrier of remote-observing traffic. The tremendous advances in bandwidth and number of users, and more important, the fact that Internet is still "free", makes it the obvious first candidate to implement the communication link. The World-Wide Web gives a convenient interface which is already used for some robotic telescopes. Internet has proven reliability, and propagation delays are in most cases acceptable. A future commercialisation of Internet may make some of the advantages obsolete.

For observatories located in remote places it may be difficult to obtain a fast Internet access. As an alternative, dedicated links to more populated areas with Internet access can be acquired. Although dedicated links are more expensive, they also offer advantages like guaranteed bandwidth and propagation delays.

There are two different techniques for gaining remote access:

- *Remote Observing Centre* – A dedicated geographical site from where the observation is carried out. This is typically located in a major astronomical research institute and the remote observer has to travel to this site. The advantages are that expert knowledge, similar to a local observatory, can be built up in order to provide accurate support to the visiting astronomer.

- *Distributed Remote Observing* – Any site with a network connection, normally Internet, can perform remote observing. The obvious advantage is that no travel is required. However, it assumes that the remote observer has expert knowledge, in order to perform efficient observation.

5. ESO Experience

ESO currently supports *active remote observing* with two telescopes. The 1.4-m CAT has been operated routinely in active remote observing mode about 50% of the time for the last six years. The NTT was the first ESO telescope designed to accommodate remote observing. Remote ob-

TABLE 2. COMPARING OPERATIONAL COST.

Monthly cost (kDM)	0% RO 0 r.ope	10% RO 1 r.ope	30% RO 2 r.ope	50%RO 2r.ope	100%RO 3 r.ope
1 tel. 5 runs/month	20	46	53	50	52
1 tel. 10 runs/month	40	61	68	62	56
1 tel. 20 runs/month	80	102	100	86	64
CAT/NTT 7+13 runs/m.	80	102	100	86	64
	0 r.ope	1 r.ope	3 r.ope	4 r.ope	6 r.ope
4 tel. 20 runs/month	320	322	291	250	142

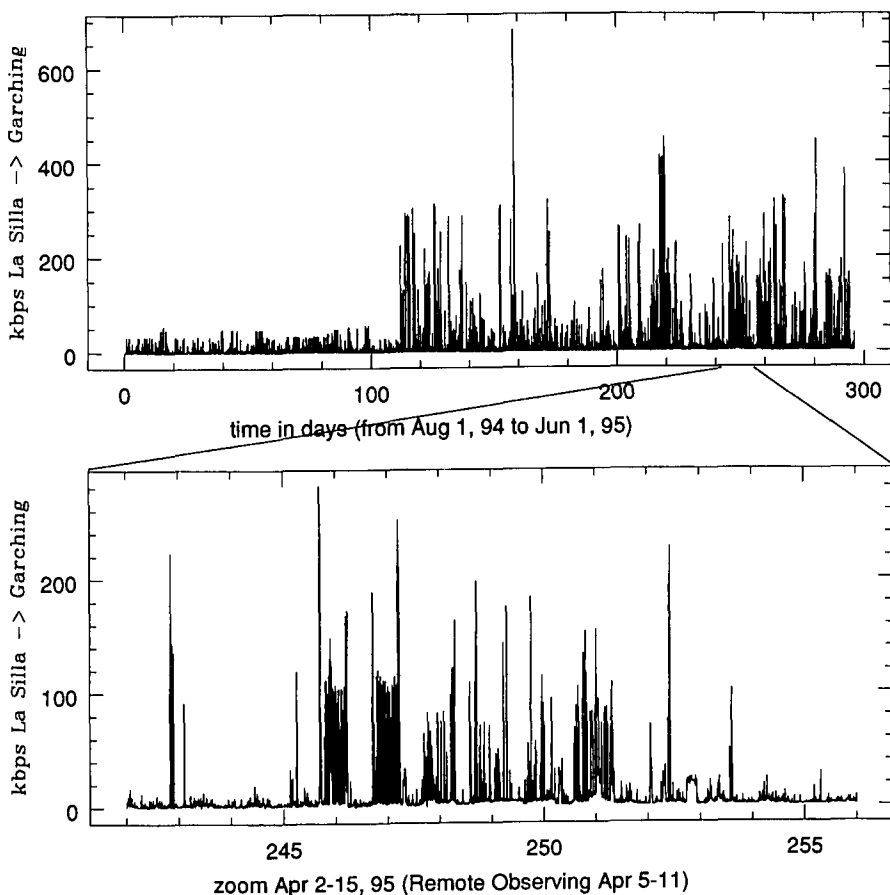


Figure 1: *Link Utilisation.*

servicing was first offered to the user community in 1993, and since then about 15% (four to five nights per month) of the time is scheduled in active remote observing mode. Early experiences with the system are described in Balestra et al. (1992), Baade et al. (1993) and Wallander (1994).

The architecture of the NTT remote observing system was reported in detail in Tucson (Emerson and Clowes, 1993), and will not be repeated here. We only summarise the main parameters. At ESO Headquarters in Garching a *Remote Observing Centre* provides the interface for remote observers to the La Silla Observatory in Chile. Observing from other sites and institutes is not supported. A dedicated satellite link provides the bandwidth between the two sites. The system provides fully interactive *active remote observing* based on dedicated remote software executing at the remote site.

During the course of 1993 and 1994, the ESO executive identified the poor communication between ESO Headquarters and the Observatory as a main obstacle for success in the VLT era. In order to overcome this and to achieve a fully integrated environment between the two sites and different activities, it was decided, among other things, to invest in a high-bandwidth communication network. This upgrade was not driven by remote observing.

In November 1994 the 64 kbps (used by NTT) and the analogue (used by CAT) PTT-leased communication links were replaced with a 2 Mbps “roof-to-roof” satellite link. The complete system was obtained as a turn-key project from an external contractor. Although this involved a considerable capital investment, the actual operation costs did not increase. It turned out that by leasing the bandwidth directly from the satellite provider, instead of via national PTT’s, a 26-fold increase in bandwidth could be acquired for a lower price. In addition, by mounting the antennas directly on the ESO premises and becoming independent of PTT’s, the reliability of the link increased. During the period November 1994 to June 1995 the availability of the link has been over 99.8%. This should be compared to the record of the previous 64 kbps PTT leased line, which in the period 1991 to 1994 had an average availability of 95%.

Figure 1 shows the data transfer rate from La Silla to Garching, averaged every

five minutes, over the last ten months. The saturation of the previous 64 kbps link, of which 32–48 kbps was allocated for data, is clearly visible. The zoom of the first two weeks of April shows that remote observing is a main, but not the only, user of the link.

Initially, the new link did not boost the data-transfer rate as expected, because the operating systems did not support the high value of the bandwidth–propagation-delay product. We obtained a patch from the supplier, which allowed us to increase the TCP window size from 8 to 32 kbytes. The next version of the operating system will allow us to increase this further. With the present patch, transferring a full $2k \times 2k$ CCD image takes about 2 minutes, or less if one accepts lossy data compression. We find that this delay is acceptable: it is already much less than the read-out time of the CCD. It is still important to start a new exposure as soon as the old one is finished, rather than first wait for the image to appear on the remote system. Observers who use the latter approach have noticeably lower efficiency.

6. Observing Efficiency

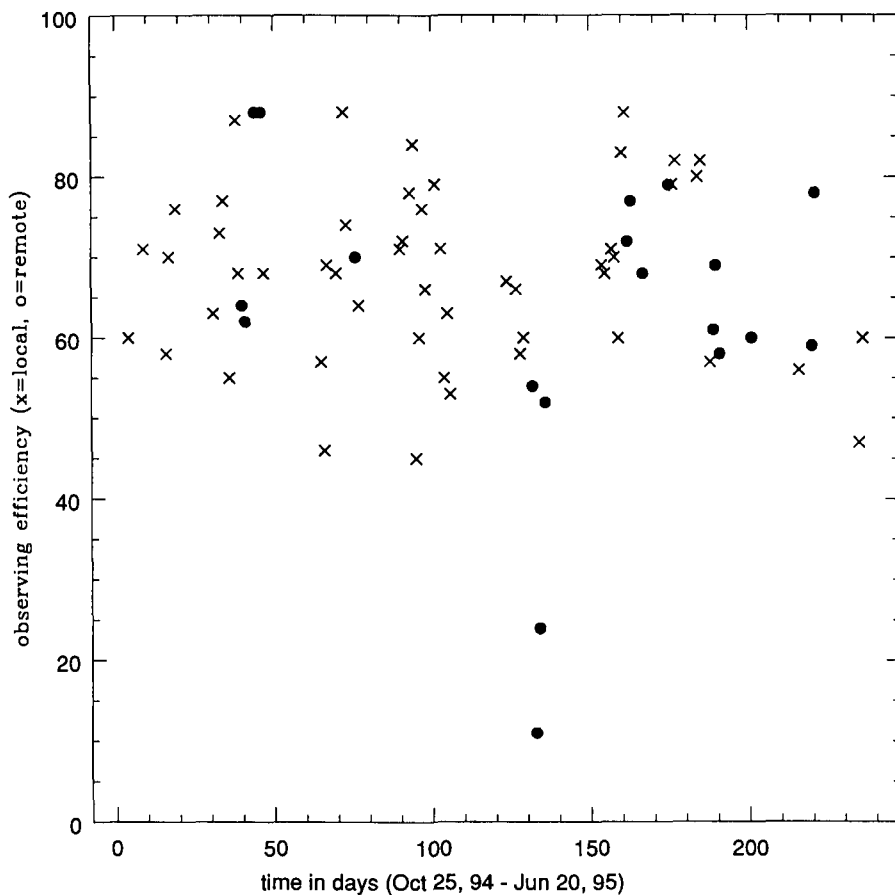
We define the observing efficiency as the fraction of the time between nautical twilights that the shutter of the instrument is open. This number is derived from the computer-based operation log and we have routinely measured it for the NTT since November last year. We only used data from nights without any technical problems or time lost for weather, and where the instrument, EMMI or SUSI, was used in one of the standard modes (we have left out MOS which is not done remotely, and dichroic observations which can have efficiencies over 100%). The result is shown in Figure 2.

With the exception of one remote observing run (2 nights) the obtained efficiency for classical and remote observing is very similar. Performing some statistics on the data, we get the result shown in Table 3. The first night of a run is listed separately because of possible familiarisation effects (“first night syndrome”), which are indeed present.

The first number gives the efficiency expressed as a percentage, with the standard deviation. The number in braces gives the number of nights used in the

TABLE 3. COMPARING CLASSICAL AND REMOTE OBSERVING EFFICIENCY.

Classical observing		Remote observing	
First night	Later nights	First night	Later nights
64+/-11% (22)	71+/-10 (29)	60+/-18 (11)	67+/-18 (8)
		65+/-10 (10)	73+/-9 (7)



the night assistant at La Silla, but it has been done remotely as well. This took 30 seconds longer and gave the same answer.

The most serious argument used by astronomers is that their object is very faint and that it is difficult to position it at the slit. If the object is not visible on the video screen, it is necessary to take acquisition images and to move the telescope such that the selected object falls in the slit. Sometimes two such exposures are needed. The additional overhead becomes larger if the science exposures are relatively short and there are many targets: if too many acquisition images need to be taken, the observer should go to La Silla.

Finally, multi-object spectroscopy is a special case: first the positioning of the telescope may be rather delicate (although here it helps that it is possible to take a direct image through the slit), but more important is the effort it takes to prepare the mask. This is generally done in the afternoon, but the software needed for this is so far only available at the telescope, and help by a technician with access to EMMI may be needed. We do not at the moment accept MOS runs for remote control.

9. Eavesdropping

So far we have not discussed *eavesdropping*. The system at the NTT allows for this as well (in fact it should be possible to implement this option for all telescopes on La Silla). If the true observer is at the telescope, and all the eavesdropper does is to help in analysing the data, there is little that can go wrong and the gain could be significant. We find that few observers have the time and energy to do a thorough analysis of their data while observing (which is a good reason why so many remote observers come in pairs). In view of this, surprisingly little use has been made of this facility at ESO, possibly because of a lack of awareness. It is also possible that the eavesdropper is the real observer, who instructs the person at the telescope what to do. In that case all of the above on remote observing applies, with the disadvantage that there is another delay when the eavesdropper communicates back to the person at the telescope, but with the advantage that he doesn't

have to bother trying to find out how to operate the instrument. At ESO we have no experience with this.

10. Future

What is the future of remote observing? There is clearly a demand from the user community, seeing that a third of the optical NTT proposals request this mode. Part of this may be due to the fact that it is easier to come with more than one person in this mode. The recent experience has shown that, for many programmes, remote control is competitive with local observing, being as efficient in telescope usage while giving a saving of the astronomer's time. At the same time, there is a large group of people who prefer to travel to La Silla. We will for the time being continue to offer remote observing as a service to the community, but not force it upon people. (This last statement is true for the NTT: for the CAT we do prescribe it as the normal mode.) We will try to improve the system to alleviate the doubts as expressed above.

A major upgrade of the NTT control system is being undertaken as part of the NTT Upgrade Project. The aim of this activity is on the one hand to verify the concept and software to be used for the VLT, on the other hand to provide an identical interface on the NTT for higher level operational tools, procedures and methods to be used on VLT. Using the NTT as a testbed for VLT for all these aspects is considered essential in order to operate VLT in an efficient way. It is expected that the VLT technology and software architecture will give essential performance advantages also for remote observing. Faster computers, more efficient communication protocols, on-the-fly data compression and fast data forwarding will reduce the data-transfer rate. The limiting factor of a CCD display will become the read-out time, independent of where the display unit is located.

11. Conclusions

We have shown that the observing efficiency does not degrade when using *active remote observing* for the ESO NTT as compared to classical observing. This allows more flexibility in scheduling, shorter observing programmes, long-

term monitoring programmes, and savings of astronomer's time.

However, *active remote observing* is nothing else than moving classical observing to another site. It does not address the "first night syndrome". To increase the scientific efficiency, service observing may be a more important observing mode than remote observing. The move to service observing may or may not make *active remote observing* obsolete. Assuming the service observer will be at the telescope, we would expect increased demands for *eavesdropping* capabilities. The requirements for this to be successful are a sufficiently fast link and adequate communication facilities, i.e. not much different from those of *active remote observing*. The main role of *active remote observing* may be found in the new generation of large telescopes, where the observing runs may be very short, and for astronomers in places where travel money is difficult to get.

12. Acknowledgement

Manfred Ziebell, with support from Joar Brynnel, has been responsible for the very successful installation and operation of the new satellite link. We thank Miguel Albrecht for providing the observing efficiency data. The successful operation of NTT remote observing would not have been possible without dedicated support from the whole operation crew, both at La Silla and in Garching.

References

- Baade D., et al., 1993, *The Messenger*, **72**, 13.
- Balestra A., et al., 1992, *The Messenger* **69**, 1.
- Burton M., 1995, in ASP Conf. Series, **73**, p. 559–562.
- Emerson D., Clowes R., 1993, *Observing at a Distance*, (World Scientific, Singapore).
- Loewenstein R.F., York D.G., 1986, *SPIE* **627**.
- Longair M.S., Stewart J.M., Williams P.M., 1986, *Q. J. R. Astr. Soc.* **27**, 153.
- Raffi G., Tarengi M., 1984, *The Messenger* **37**, 1.
- Raffi G., Ziebell M., 1986, *The Messenger* **44**, 26.
- Raffi G. et al. 1990, *SPIE* **1235**.
- Tyson N.D., Gal R.R., 1993, *AJ*, **105**, 1206.
- Wallander A., 1994, *Nuclear Instruments and Methods in Physics Research Vol. A347*.

E-mail address:
A.A. Zijlstra, azijlstr@eso.org

Library and Information Services in Astronomy II (LISA-II)

U. GROTHKOPF, F. MURTAGH, M. ALBRECHT, ESO

Library and Information Services in Astronomy II (LISA-II), an IAU Technical Workshop, was held at the European

Southern Observatory (ESO), Garching near Munich, Germany from May 10-12, 1995. LISA-I had been held in Washing-

ton D.C. in 1988. The aims of LISA-II were twofold: (1) to provide the opportunity for librarians of astronomical observatories

and institutes to meet to discuss common problems, and ways of stimulating greater co-operation between libraries and their services; and (2) to raise discussion about the interface areas between astronomical libraries and the wide range of on-line and other astronomical computer-based services which are becoming ever more widespread.

Various groups of people, and disciplines, were involved in LISA-II. These included, of course, those who run astronomical libraries. The astronomical library is seeing many changes. On-line and other digital information is on the increase. Wide-area telecommunication networks are commonly used for accessing and ordering new material, cross-checking references, and so on. And catalogues of library holdings are becoming automated, through DBMS-based and accompanying scanning systems.

Information science work was strongly represented. This includes information retrieval, increasingly computer network-based; indexing and searching; and the handling of information and data in very diverse forms.

Astronomers, not only those who participated, are acutely concerned with the presentation and dissemination of data and information, and ultimately knowledge.

An important part of the meeting was devoted to current evolution in electronic publishing. Representatives from many of the major publishing houses and establishments took part.

A secular trend which is quite apparent is the convergence of concerns, and often indeed of priorities, in these fields. It is always exciting to witness significant changes in the way we do things. There are attendant difficulties lurking also, especially for those who face major problems in regard to resources.

This meeting was truly international. 121 LISA-II participants from 26 countries learned about projects, research and efforts taking place all over the world.

The local organisers wish to thank colleagues at ESO for help in lots of ways, which led to a very productive meeting. The help of the many sponsors of LISA-II is gratefully acknowledged. The "Friends of LISA-II" committee (Brenda Corbin, U.S. Naval Observatory; Marlene Cummins, University of



Photograph by H.-H. Heyer

Toronto; and Ellen Bouton, NRAO) worked tirelessly to facilitate participation on a wide basis.

The proceedings of LISA-II will be published as a special issue of the journal *Vistas in Astronomy*. The volume contains a selection of papers as well as abstracts of poster contributions. Full texts of posters can be found in the LISA-II area on the World-Wide Web at URL <http://www.eso.org/lisa-ii.html>; some other "goodies" are also available on the Web, like the complete programme and the group photograph taken during the conference.

LISA-II once again has shown how important meetings of this kind are, especially to librarians, who have not always had a possibility to meet their colleagues personally in the past. The results will be manifold, be they additional information about techniques and tools in information services, closer working relationships, or higher motivation in general. We are looking forward to LISA-III which hopefully will take place in the near future.

E-mail address: esolib@eso.org

ANNOUNCEMENT

Programmes Approved for Period 56

Key Programmes

ESO No.	Names of Pls	Title of submitted programme	Telescope
143.A-0003	de Lapparent et al.	A redshift survey of galaxies with $z \leq 0.6$ using multi-slit spectroscopy	NTT
149.A-0023	Böhringer et al.	Redshift survey of ROSAT clusters of galaxies	3.6-m, 1.5-m
143.B-0007	Cristiani et al.	A homogeneous bright quasar survey	90-cm Dutch
145.B-0009	Reimers et al.	A wide-angle objective-prism survey for bright QSOs	2.2-m, 1.5-m, 90-cm Du
149.B-0013	D'Odorico et al.	A statistical study of the intergalactic medium at high redshifts	NTT
151.D-0004	Turatto et al.	A photometric and spectroscopic study of supernovae of all types	3.6-m, NTT, 2.2-m
149.E-0002	Epchtein et al.	Deep near-infrared survey of the southern sky (DENIS)	1-m

ESO No.	Names of Pls (in alphabetical order)	Title of submitted programme	Telescope(s)
C-0396	Ageorges/Eckart/Quirrenbach/Fisher	Sharp imaging and polarimetry of reflection nebulae associated with young stellar objects	NTT
E-0601	Alcala/Bouvier/Covino/Krautter/Magazzù/Martin/Terranegra/Wichmann	Study of the evolution of lithium and rotation in low-mass pre-main sequence stars	3.6-m
E-0566	Alcala/Sterzik/Neuhauser/Schmitt/Covino/Magazzù/Martin	A search for young disk-population stars from the ROSAT All-Sky Survey	1.5-m
A-0378	Andreani/La Franca/Miller/Cristiani/Lissandrini	The cosmological evolution of the clustering of quasars	3.6-m
E-0198	Antonello/Mantegazza/Poretti	Cepheids in the nearby galaxy IC 1613	0.9-m Du
E-0641	Ardeberg/Gustafsson/Linde/Nissen	Chemical evolution and star formation in LMC – calibration of HST	2.2-m
F-0012	Arlot/Thuillot/Bouchet/Colas/Descamps/Sicardy/Vu	Observation of the events of the satellites of Saturn	0.5-m
D-0730	Augusteijn/Rutten/van Paradijs/Abbott	A comparative study of disk and halo cataclysmic variables	0.9-m Du
D-0772	Augusteijn/van den Heuvel/Kahabka	Phase-resolved spectroscopy of the supersoft X-ray binary CAL 87	NTT
D-0728	Augusteijn/van Paradijs	IR photometry of the exceptional dwarf nova V485 Cen	2.2-m
D-0361	Azzopardi/Breysacher/Muratorio/Testor	Wolf-Rayet stars in NGC 300: completion of the survey and spectroscopic study	NTT
E-0346	Azzopardi/Breysacher/Muratorio/Westerlund	Carbon star luminosity function of the Fornax dwarf spheroidal galaxy	3.6-m, 2.2-m
D-0381	Baade/Kaufer/Stahl/Steffl/Wolf	Line profile and Balmer discontinuity variations in Be stars	0.5-m
B-0529	Bade/Voges/Fink	An X-ray variability selected sample of AGN	1.5-m D
E-0323	Barbuy/Maeder/De Medeiros	CNO in yellow supergiants	1.4-m CAT
E-0590	Barbuy/Schiavon	Near-infrared features in cool stars and globular clusters	1.5-m
B-0113	Barthel/Hes/Douglas/de Vries	The high-redshift nature of GSP radio sources: searching for distant quasars and radio galaxies	3.6-m
F-0468	Barucci/Fulchignoni/Lazzarin/Dotto/De Sanctis/Doressoundiram	Study of the chemical properties of asteroids 3837 CARR, 5224 ABBE, 5642 1990 OK1, 1983 AD and 4258 Ryza-nov: possible Rosetta targets	1.5-m
A-0680	Beaulieu/Ferlet/Grison/Vidal-Madjar/Ansari/Aubourg	Can an intrinsic extremely rare phenomenon mimic microlensing effects ?	3.6-m
C-0500	Benvenuti/Porceddu	Dibs toward high-latitude molecular clouds	1.4-m CAT
A-0684	Bertola/Cinzano/Corsini/Pizzella	A study of the disk and bulge kinematics in late-type spirals	1.5-m
A-0672	Beuing/Bender/Saglia/Döbereiner	Influence of the stellar population on X-ray properties of ellipticals	1.5-m
E-0545	Blommaert/Groenewegen/Josselin/van der Veen/Omont	CO, HCN and SO observations of late-type supergiants	SEST
C-0511	Bocchino/Sciortino/Maggio/Favata/Raymond	Testing the emission conditions of selected filaments of the Vela supernova remnant (SNR).	2.2-m
F-0133	Bönnhardt/Käuffl	Investigation of a potential target comet of the ESA Rosetta mission: P/Schwassmann-Wachmann 3 as representative of the Jupiter family comets	3.6-m, NTT
E-0202	Bouvier/Wichmann/Allain	Coyotes V: accretion columns in T Tauri stars	0.9-m Du
D-0231	Bragaglia/Munari/Oswalt	Spectroscopic study of binary systems containing a white dwarf: pre-cataclysmics and double degenerates	1.5-m D
F-0808	Brahic/Ferrari/Lagage/Rotundi/Thebault	Saturn's rings edge-on observations	1.5-m D
A-0713	Bremer/Hes/Barthel/Baker	The cluster environment of radio loud quasars	2.2-m
A-0350	Bresolin	Stellar populations in spiral galaxies along the Hubble sequence	1.5-m D

ESO No.	Names of PIs (in alphabetical order)	Title of submitted programme	Telescope(s)
E-0220	Brocato/Ferraro/Testa/Castellani/ Piersimoni	The age of old Magellanic Cloud clusters	NTT
C-0615	Bronfman/Israel	Translucent cloud veiling the galaxy NGC 6822	SEST
E-0395	Bues/Aslan/Karl-Dietze	Magnetic changes of abundances in very cool white dwarfs	1.5-m
D-0561	Burwitz/Beuermann/Reinsch/Schwope/ Thomas	The orbital period distribution of AM Herculis binaries	0.9-m Du
A-0373	Butcher/Poggianti/Couch/Dressler/Ellis/ Oemler/Sharples/Smail	Spectroscopy of Butcher-Oemler cluster galaxies	NTT
B-0175	Carrillo/Courvoisier/Paltani/Walter	Near-infrared and millimetric photometry of a quasar sample	SEST
E-0321	Castellani/Bono/Brocato/Caputo/Davis/ Degl'Innocenti/Marconi/Piersimoni/ Ripepi/Stellingwerf	Variable stars in dwarf spheroidal galaxies: Leo I, Leo II and Sextans	1.5-m D
C-0509	Castets/Duvert	Molecular outflow from FU Orionis star Z CMA	SEST
E-0785	Cayrel/Nissen/Beers/Spite/Spite/ Andersen/Nordström/Barbuy	Survey of very metal-poor stars in the Galaxy	NTT
B-0722	Chatzichristou/Miley	The origin of mid-IR excess in extreme warm IRAS Seyferts: IR tracers of recent interactions?	1.5-m D
C-0108	Chin/Henkel/Whiteoak/Osterberg/Hunt	Molecular abundance in N113: the brightest region in Magellanic Clouds	SEST
C-0105	Chin/Henkel/Whiteoak/Osterberg/Hunt	Molecular investigation of the LMC region N214DE	SEST
C-0118	Chin/Whiteoak/Henkel/Hunt/Lemme	Molecular abundances in the Small Magellanic Cloud	SEST
A-0463	Chini/Krügel	Determination of the conversion factor CO:H ₂ in spiral galaxies	SEST
A-0419	Chiosi/Vallenari/Bertelli/Bressan	Star formation in dwarf galaxies: the Fornax	2.2-m
D-0415	Chiosi/Vallenari/Bertelli/Girardi	Photometry of unstudied clusters in the LMC bar	NTT
D-0156	Christensen-Dalsgaard/Weiss	Asteroseismology of solar-type stars	1.5-m D
A-0180	Collins/Burke/Bohringer/Neumann/ Nichol	A distant sample of X-ray selected galaxy clusters	3.6-m
A-0487	Combes/Casoli/Horellou	NGC 7252: the fate of returning HI gas in mergers	SEST
F-0711	Combes/Vapillon/Coustenis/Gendron/ Encrenaz/Dumas/Lai	Spectro-imagery of the surface and atmosphere of Titan with Adonis	3.6-m
B-0391	Contini/Davoust/Considère	Search for Wolf-Rayet stars in very young starburst galaxies	1.5-m
D-0299	Corporon/Lagrange/Böhm	A search for spectroscopic binaries among Herbig stars	1.4-m CAT
A-0746	Côté /Skillman/Miller	An H α imaging survey of Sculptor dwarf galaxies	1.5-m D
C-0731	Cumming/Lundqvist/Sollerman/ Fransson	Spectrophotometry of Supernova 1987A's triple-ring nebula	NTT
B-0789	D'Odorico/Cristiani/Fontana/Giallongo/ Savaglio	Ultra-high-resolution spectra of absorption lines in quasar spectra: how low is the gas temperature in the IGM?	NTT
C-0333	Danks/Sembach/Caulet/Perez	High velocity gas in the Vela supernova remnant	1.4-m CAT
C-0379	Danziger/Barlow/Liu/Storey	Benchmark CNO abundances for H II regions in the Magellanic Clouds from optical recombination lines	NTT
D-0362	Danziger/Bouchet/Lucy/Fransson/ Mazzali/Della Valle/Chugai/Benetti	SN 1987A	3.6-m, 2.2-m
A-0458	Danziger/Carollo	Formation/evolution of ellipticals: fundamental plane as function of redshift	NTT
A-0493	De Grandi/Molinari/Böhringer/ Chincarini	Photometric properties of X-ray-selected clusters of galaxies	1.5-m D
A-0782	de Lapparent/de Lapparent/ Rocca-Volmerange/Arnouts/Fioc	Deep K' photometry for the ESO-Sculptor faint galaxy redshift survey	2.2-m
D-0359	De Mey	Eta Orionis	1.4-m CAT
D-0441	Della Valle	Spectroscopy of galactic novae at late stages	1.5-m
D-0674	Della Valle/Giavalisco/Livio/Perlmutter/ Pain/Goobar	A search for supernova events in high-redshift galaxies	NTT
F-0371	di Martino/Zappalà/Cellino/Miglorini/ Barucci	Spectroscopic observations of family asteroids	1.5-m
B-0696	di Serego Alighieri/Cimatti/Fosbury/ Manzini/McCarthy/Villani	The nature of the rest-frame UV continuum in radio galaxies	3.6-m, 2.2-m
B-0286	Dietrich/North/Wagner/Courvoisier	Counting broad-line region clouds with high-resolution spectroscopy	NTT
A-0827	Doublier/Comte/Caulet	B, V and R photometry of blue compact dwarf galaxies at $z \leq 0.02$	1.5-m D
A-0834	Doublier/Comte/Caulet/Kunth/ Mas-Hesse/Petrossian	Infrared imaging of starburst galaxies	2.2-m
A-0285	Dubath/Queloz/Smecker-Hane/Stetson/ Hesser	Search for dark matter in the Carina dwarf spheroidal galaxy	NTT
A-0757	Duc/Mirabel	Star population in tidal dwarf galaxies	2.2-m
D-0724	Duerbeck/Covarrubias	A search for the old (hibernating?) Nova Puppis 1673	0.9-m Du
A-0524	Eckart/Eisenhauer/Sams/Tacconi- Garman/Genzel/Hofmann	Speckle-spectroscopic imaging of the galactic centre	NTT
A-0517	Eckart/Genzel/Sams/Tacconi-Garman/ Hofmann	Proper motions in the Galactic centre	NTT
B-0153	Falomo/Kotilainen	Near-infrared imaging of flat-spectrum radio quasars	2.2-m
B-0330	Falomo/Ulrich	Properties of the galaxies hosting the BL Lac objects	NTT
B-0152	Fasano/Falomo/Scarpa	The optical properties of a complete sample of radio galaxies	1.5-m D
E-0149	Favata	The lithium abundance of metal poor K dwarfs	1.4-m CAT
A-0250	Felenbok/Durret/Gerbal/Lobo/Slezak/ Mazure	Structural analysis of two rich X-ray clusters of galaxies. I. Spectroscopy	3.6-m
E-0610	Feltzing/Gustafsson/Heyn Olsen	The metal-rich galactic disk population	1.4-m CAT

ESO No.	Names of PIs (in alphabetical order)	Title of submitted programme	Telescope(s)
C-0812	Fernandes/Tedds/Brand/Burton/ Ramsay-Howatt	Adonis H ₂ and [Fe II] imaging of shock fronts in Orion bullets	3.6-m
E-0548	Ferrari/Bucciarelli/Massone/Lasker/ Postman/Le Poole/Lattanzi	Photometric calibrators for the southern sky surveys	0.9-m Du
E-0376	Festini	Deep CCD photometry for determination of the IMF for the latest M-dwarfs	NTT
A-0414	Fort/Mellier/Kneib/Huepe	Detection and measurement of gravitational shear around magnified radio sources	NTT
A-0702	Franx/Kuijken/Sackett/Fisher/Squires	The mass distribution of groups of galaxies from weak lensing	NTT
A-0456	Freeman/Arnaboldi/Capaccioli/Ford/ Gerhardt/Hui/Kudritzki/Méndez/ Quinn	Will late-stage merger systems with an $r^{1/4}$ luminosity profile + disturbed envelope form CD giants?	NTT
F-0465	Fulchignoni/Barucci/Dotto/di Martino/ De Sanctis/Doressoundiram	Slow rotator asteroids: implications on the collisional evolution of the small bodies population	0.9-m Du
D-0460	Fullerton/Glatzel/Fricke/Schneider/Puls	A spectroscopic search for pulsational variability in massive O3 stars	3.6-m
E-0139	Geffert/Tucholke/Odenkirchen	Globular cluster proper motions from deep CCD astrometry	1.5-m D
E-0422	Gemmo	An infrared search for companions to white dwarfs.	2.2-m
D-0515	Gemmo/Cristiani/La Franca/Andreani	The luminosity function of hot white dwarfs	1.5-m
F-0420	Gemmo/Hainaut/Barbieri/Standish	Improving the ephemeris of Pluto: long-term CCD astrometry	1.5-m D
D-0513	Gerbaldi/Faraggiana	Abundances of high galactic latitude and apparently young stars	NTT
D-0581	Gilmozzi/Panagia/Kinney/Ewald/Shara/ Scuderi	Population content in young, globular-like clusters in the LMC	NTT
B-0734	Giraud/Van de Steene	A protocluster candidate around a radio galaxy at $z = 2.47$	3.6-m, NTT
E-0484	Gratton/Carretta/Snedden	Mixing episodes during the RGB evolution of metal-poor stars	1.4-m CAT
D-0439	Grebel/Brandner/Roberts	Blue giants and the main-sequence turn-off in young Magellanic Cloud clusters	2.2-m
C-0701	Gredel/Dalgarno	X-ray excited molecular hydrogen emission around T Tau stars	NTT, 2.2-m
E-0325	Groenewegen/Blommaert/Omont	A study of mass-losing AGB stars in the Small Magellanic Cloud	2.2-m
B-0607	Grupponi/De Ruiter/Marano/Mignoli/ Zamorani	Optical identification of faint radio sources in the "Marano Field"	3.6-m
E-0578	Gustafsson/Asplund/Lambert/Rao/ Eriksson	Infrared spectroscopy of R Coronae Borealis stars	NTT
B-0544	Hasinger/Schwope/Voges/Trumper/ Fischer/Boller	Interaction and galaxy activity in a complete sample of bright ROSAT AGN	2.2-m
D-0659	Heber/Dreizler/Haas/Drilling/Beers/ Wisotzki	Scale height, space density and birth rate of SdB stars	1.5-m
A-0538	Held/Piotto/Saviane	The giant and horizontal branches of the Fornax dwarf spheroidal	1.5-m D
C-0120	Henkel/Chin/Whiteoak/Mauersberger	Galactic oxygen isotope ratios: are they correct?	SEST
C-0104	Henkel/Chin/Whiteoak/Tieftrunk/Wilson	Oxygen burning in massive stars: the Galactic centre region	SEST
B-0488	Henkel/Schulz	Optical spectroscopy of H ₂ O Megamaser sources	1.5-m
C-0275	Henning/Launhardt	Towards the structure of extreme class I sources	SEST
D-0157	Heydari-Malayeri/Beuzit	Are there stars with a mass over 100 M _⊙ in the Magellanic Clouds?	3.6-m
E-0703	Hoff/Alcala/Pfau/Henning	Search for pre-main sequence stars around isolated T Tauri stars	1.5-m
E-0209	Holweger/Krege/Rentzsch-Holm	High-resolution spectroscopy of dusty and dust-free A stars	1.4-m CAT
D-0652	Hurley/Smith/Durouchoux/Waters/van Paradijs/Schultz/Wallyn	Millimetre observations of the soft Gamma-ray repeater counterparts	SEST
A-0527	Jaffe/Bremer/v.d. Werf/Johnstone	H ₂ emission from central cluster galaxies: diagnostic of cooling flows or AGN?	NTT
E-0643	Jørgensen/Hron/Kerschbaum/Aringer	The atmospheric ¹² C/ ¹³ C ratio of semiregular and Mira variables	NTT
E0621	Josselin/Loup/Omont/Barnbaum	The nature of IRAS sources with a CO deficit	1.5-m
D-0252	Kaper/Baade/Fullerton/Gies/Henrichs/ Puls	A search for cyclical variability in O-star winds (summer targets)	1.4-m CAT
D-0499	Kaper/Carraro/Patà/Zijlstra	The most luminous stars in the Large Magellanic Cloud	1.5-m D
B-0605	Kelm/Reduzzi/Rampazzo/Longhetti/ Palumbo	Seyfert galaxies in a complete sample of southern isolated pairs	1.5-m
C-0165	Köppen/Rauch/Werner	Expansion velocities of highly excited planetary nebulae	1.4-m CAT
D-0162	Koester/Reimers/Schönberner	White dwarfs in NGC 3532 and the initial-final mass relation	3.6-m
A-0588	Kohle/Schneider	Local standard stars for refinement of the cosmological distance ladder	0.9-m Du
E-0117	Krautter/Pasquini/Metanomski/Schmitt	Nature of late-type stars in the ROSAT All-Sky Survey	0.5-m
E-0483	Kürster/Cutispoto/Schmitt	Towards Butterfly diagrams for active stars	1.4-m CAT, 0.5-m
E-0490	Kürster/Hatzes/Cochran/Dennerl/ Döbereiner	High-precision stellar radial velocities, Part VII	1.4-m CAT
B-0388	La Franca/Cristiani/Andreani/Gemmo	The completion of the homogeneous bright QSO survey at $b < 17$	1.5-m
F-0355	Lagerkvist/Dahlgren/Lahulla/Williams/ Fitzsimmons	Compositional studies of Cybele asteroids by spectroscopy	NTT
F-0525	Lagerkvist/Erikson/Magnusson/ Piironen/Dahlgren	Physical properties of asteroids with long rotational period	0.5-m, 0.9-m Du
E-0342	Lagrange/Mouillet/Beust/Vidal-Madjar/ Ferlet/Lecavelier/Deleuil/Tobin	Long-term high-resolution spectroscopic survey of β Pictoris with the CES	1.4-m CAT

ESO No.	Names of PIs (in alphabetical order)	Title of submitted programme	Telescope(s)
E-0343	Lagrange/Mouillet/Beuzit/Vidal-Madjar/ Lecavelier/Colas	Coronagraphic observations of the disk with adaptive optics	3.6-m
C-0510	Launhardt/Henning/Bourke	Detailed study of five protostellar cores in southern globules	SEST
C-0264	Launhardt/Zinnecker/Henning/Stecklum	Binary and multiple star formation in isolated Bok globules	3.6-m
A-0402	Le Fèvre/Crampton/Deltorn/Dickinson	Clustering of galaxies around 3CR radio galaxies with $0.8 \leq z \leq 1.4$	NTT
A-0225	Leibundgut/Hamuy/Maza/Phillips/ Schommer/Smith/Suntzeff/Spyromilio/Schmidt/Kirshner/Riess	Spectroscopy and photometry of distant supernovae	NTT, 1.5-m D
E-0197	Leinert/Zinnecker/Eckart/Alcala	The binary frequency of weak-lined T Tauri stars in Chamaeleon	NTT
E-0648	Leisy/Alard	Photometric calibration for LMC and SMC survey	1.5-m D
C-0806	Leisy/Dennefeld	Accurate abundances in selected planetary nebulae of the Magellanic Clouds	1.5-m
D-0504	Lennon/Rosa/Kudritzki/Hopp/Venn/ Herrero	Multi-object spectroscopy of luminous stars in galaxies beyond the Local Group: NGC 5253	NTT
A-0449	Lidman/Colless/Glazebrook	Deep infrared survey of $b < 24$ redshift survey galaxies	2.2-m
E-0004	Liller/Alcaíno/Alvarado/Samus	UBVRI CCD photometry of Magellanic Cloud cluster standards	0.9-m Du
C-0577	Lioure/Smith/Davis	A systematic study of molecular hydrogen in OMC-1	
C-0380	Lorenzetti/Vitali	Small-scale mass outflows in the Vela star-forming region	2.2-m
E-0800	Loup/Blommaert/Epchtein/Forveille/ Fouqué/Groenewegen/Guglielmo/ Josselin/Le Bertre/Omont/Persi/ Zijlstra	Unidentified infrared sources in 30 Doradus	2.2-m 2.2-m
E-0740	Loup/Hron/Kerschbaum/van Loon/ Omont/Trams/Waters/Zijlstra	The spectral type of mass-losing AGB stars in the LMC	1.5-m D
A-0329	Maccagni/Chincarini/Garilli/Infante/ Iovino/Quintana/Saracco	Redshift distribution of a complete, magnitude limited, K-selected galaxy sample	NTT
A-0614	Macchetto/Caon/Pastoriza/Sparks/ Bender/Capaccioli	Long-slit spectroscopy of gas-rich elliptical galaxies	3.6-m
A-0430	Macchetto/Giavalisco	A search for primeval galaxies in the redshift range $3 < z < 3.5$	NTT
E-0244	Maceroni/van 't Veer/Vilhu	Magnetic activity and secular evolution of late-type contact binaries	1.4-m CAT, 0.5-m
E-0384	Magain/Hammida/Zhao	Cosmic scatter of heavy elements in halo stars	1.4-m CAT
E-0668	Malbet/Bertout/Léna/Tessier/Eisöföfel	Multi-wavelength infrared imaging of the extended structure around Z CMa with Adonis	3.6-m
B-0230	Manfroid/Gosset/Royer/Moreau	A multi-technique quasar survey: extension of the calibration of the UBVRI survey	1.5-m D, 0.9-m Du
B-0344	Marco/Alloin/Rouan	Near-infrared spectroscopic imaging of active galactic nuclei at a resolution of $0.3''$	3.6-m
D-0409	Marconi/Lennon/Mazzali/Baade/Pasian	Infrared photometry of NGC 330 in SMC and NGC 2004 in LMC	2.2-m
B-0144	Márquez/Durret	Analysis of the sufficient conditions for the onset of activity in galactic nuclei of spirals	1.5-m
B-0557	Márquez/Durret/Petitjean	Morphology of galaxies hosting quasars with extended ionised envelopes	2.2-m
C-0432	Marx/Bomans/Chin/Mebold/Zimmer/ Herbstmeier	CO investigation of very cold clouds in the LMC	SEST
A-0814	Masegosa/Bergvall/Moles/Olofsson/ Östlin/Melnick/Rönback/Hidalgo-Gamez	Helium abundances in low-metallicity galaxies	2.2-m
E-0690	Mathys/Hubrig/Landstreet/Lanz/ Manfroid	Magnetic field geometry in Ap stars with magnetically resolved lines	3.6-m
E-0688	Mathys/Hubrig/Landstreet/Lanz/ Manfroid	Systematic search and study of Ap stars with magnetically resolved lines	1.4-m CAT
E-0694	McCaughrean/Zinnecker/Leinert/ Stauffer	Binarity in the Trapezium cluster	3.6-m
A-0401	Mellier/Ellis/Fort/Kneib/Smail	Mass components in rich clusters: combining weak shear mapping of the cluster halos with giant arc modelling of the cores	NTT
A-0442	Melnick/Terlevich/Terlevich/Hansen- Ruiz	Spectrophotometry of high-redshift HII galaxies	3.6-m, NTT
B-0496	Merck/Mücke/Pohl/Radecke/Rupprecht	Correlated optical photometry of the brightest EGRET blazars	0.9-m Du
E-0393	Mermilliod/Mayor	Constraints on stellar formation from orbital elements of cluster binaries	1.5-m D
A-0110	Meylan/Azzopardi/Dubath/Lequeux	Search for dark matter in the Fornax dwarf spheroidal galaxy	NTT
B-0600	Miley/Röttgering/van Ojik	High-resolution study of the ionised gas in $z > 2$ radio galaxies	NTT
A-0353	Minniti/Bedding/Sams/Fosbury	Infrared colour-magnitude diagrams for the brightest stars in NGC 5128 (= Cen A)	3.6-m
E-0472	Minniti/Kotilainen/Zijlstra/Alonso	The bright stellar population in NGC 300	2.2-m
B-0454	Morganti/Tadhunter	Understanding the physical basis of the optical/radio correlations for radio galaxies	2.2-m
D-0241	Munari/Zwitter	Spectrophotometric survey of candidate cataclysmic variables	1.5-m
D-0569	Najarro/Herrero/Lennon/Kudritzki	IR spectroscopy of Galactic early-type stars undergoing mass loss	NTT
E-0665	Nissen/Schuster	Chemical composition of halo and thick-disk stars with overlapping metallicities	NTT
E-0640	North/Polosukhina/Lyubimkov	Lithium in cool Ap stars	1.4-m CAT
D-0761	Nota/Clampin/Leitherer/Pasquali	Spectroscopy and coronagraphic imaging of LBV candidates	NTT

ESO No.	Names of PIs (in alphabetical order)	Title of submitted programme	Telescope(s)
A-0795	Oliveira	Dwarfs in clusters of galaxies	3.6-m, 1.5-m D
E-0188	Origlia/Fusi Pecci/Ferraro	Mid-IR imaging of IRAS sources in galactic globular clusters	3.6-m
C-0189	Origlia/Gredel/Fusi Pecci/Ferraro	Millimetre CO mapping of galactic globular clusters	SEST
E-0210	Pallavicini/Pasquini/Molaro	Lithium in turn-off stars of the old metal-poor open cluster NGC 2243	3.6-m
E-0281	Pallavicini/Randich/Pasquini	Lithium and chromospheric activity in tidally locked binaries	1.4-m CAT
E-0351	Pasquini/Molaro/Castelli	Be ⁹ abundance in solar-type stars	3.6-m
B-0261	Petitjean/Bergeron/Rauch/Weymann	High-redshift OVI absorbers: a collisionally ionised phase?	3.6-m
A-0636	Petitjean/Smette/Surdej/Shaver/ Mücket/Remy	Structure of the Universe at low z from the Ly α gas	NTT
E-0809	Pettersson	RIJHK photometry of YSOs in the Vela molecular ridge	0.9-m Du
C-0535	Pfau/Henning/Maier	Testing carbon-chain molecules as absorbers of diffuse interstellar bands	1.4-m CAT
A-0540	Pierre/Mellier/Soucail/Liang/Böhringer/ Hunstead	Dynamical study of massive distant X-ray clusters	3.6-m
E-0308	Poretti/Mantegazza/Bossi/Zerbi/ Rodriguez/Koen/Martinez/Krisciunas	Search for g-mode pulsators among early F-type main-sequence stars	1.4-m CAT, 0.5-m
A-0406	Proust/Maurogordato/Cappi/Le Fèvre/ Vanderriest	Dynamics and hidden mass in two rich and X-ray luminous clusters of galaxies	3.6-m
A-0207	Proust/Quintana/Fouqué	Structure and dynamical evolution in clusters of galaxies	1.5-m
C-0553	Quirrenbach/Bertoldi/Boulanger	Imaging infrared spectroscopy of the PIGs near θ^1 Ori C	3.6-m
D-0573	Quirrenbach/Brandl/Genzel/Zinnecker	The mass function and stellar population of NGC 3603	3.6-m
B-0611	Quirrenbach/Eckart/Tacconi-Garman/ Thatte	Adaptive optics infrared line imaging of NGC 1068	3.6-m
D-0368	Ramsay/Wheatley/Mason/Cropper	Probing the accretion flow in the MCV PQ Gem	2.2-m
D-0717	Rauch/Napiwotzki/Werner/Köppen	Spectral analyses of central stars of highly excited planetary nebulae	3.6-m
F-0464	Rauer/Bockelée-Morvan/Crovisier/lp/ Thomas	Observations of Chiron and the inner coma ion distribution in Comet P/Honda-Mrkos-Pajdusakova	2.2-m
B-0228	Reimers/Köhler/Lopez/Smette	Absorption lines in the new double quasar He 1104-1805 AB	NTT
D-0552	Reinsch/Beuermann/Burwitz/Thomas	Time-resolved spectroscopy of two new eclipsing AM Herculis systems	2.2-m
E-0715	Reipurth	The youngest stars	3.6-m
A-0820	Rönnback	A search for extended low-surface-brightness disks	0.9-m Du
B-0171	Röser/Meisenheimer/Neumann	Particle acceleration regions in the jet of 3C 273	3.6-m
A-0804	Rosati/Burg/Giacconi/McLean/Della Ceca	Imaging and spectroscopy of a faint X-ray-selected cluster sample	3.6-m
C-0360	Rouan/Lai/Field/Lemaire/Falgaronne/ Rostas	Small-scale structure observed in H ₂ IR emission in the interstellar medium	3.6m
C-0618	Rubio/Garay/Lequeux	Dense gas in the Small Magellanic Cloud	SEST
D-0418	Ruiz	Luminosity function of cool white dwarfs	3.6-m
A-0352	Saglia/Bender/Jeske/Gerhard	Probing the gravitational potential and anisotropy of elliptical galaxies	NTT
A-0502	Sams/Genzel/Eisenhauer/Brandl/ Hofmann	Diffraction limited H-band studies of galaxy evolution and morphology in intermediate-redshift clusters	3.6-m
C-0537	Schild/Miller/Tennynson	Morphology and temperature structure of H ₂ outflows in OMC-1	3.6-m
D-0700	Schmutz	Observational data for hydrodynamic atmosphere models of Wolf-Rayet stars	NTT
E-0526	Schmutz/Dumm/Mürset/Nussbaumer/ Schild	Orbital elements, M giant radius, and distance of symbiotic systems	1.4-m CAT
D-0327	Schmutz/Kaufer/Stahl/Wolf	Observational constraints on the ionisation structure and velocity law in WR binaries	0.5-m
D-0179	Schönberner/Herwig/Koester/Reimers/ Rendtel	Cluster parameters, white dwarfs and the initial-final mass relation:	1.5-m
E-0774	Schwarz/Nyman/van der Blik/ Eriksson/Gustafsson	The evolutionary status of IRAS 07559-5859 and IC 2220	1.4-m CAT
B-0467	Shaver/Wall/Kellermann/Jackson	The nature of the faint flat-spectrum radio galaxies	3.6-m
D-0543	Simon/Andersen/Clausen/Maxted	Reconstruction and analysis of spectra of components of hot binaries	1.5-m D
D-0704	Smith/Waters/van Paradijs/Schultz/ Hurley	Mid-infrared observations of the soft gamma-ray repeater SGR 0525-66	3.6-m
C-0191	Sobolev/Walmsley/Zinchenko	Colliding clouds in G 1.6-0.025	SEST
E-0186	Spite/Spite/Hill	Cluster formation and abundances in the LMC	NTT
D-0334	Stell/Aerts/Balona	Modelling of fast rotation effects in line-profile variations of the Be star 28 CMA	1.4-m CAT
D-0392	Sterken/Breysacher/Maeder/Bratschi	Photometric monitoring of the W-R eclipsing binary HD 5980 in the SMC	0.5-m
D-0249	Sterken/Bruch/de Groot/Duerbeck/ Gosset/Hensberge/Manfroid/ Jorissen/Stahl/Thé/van Genderen/ Vreux/Wolf	Long-term photometry of variables	0.5-m
A-0257	Sturm	Infrared imaging and study of the evolution of dwarf galaxies	2.2-m
B-0146	Tadhunter/Morganti/Fosbury/Dickson	The stellar content of high redshift radio galaxies	3.6-m
D-0272	Testor/Niemela/Schild	Spectroscopy of bright stars in selected OB associations in LMC and SMC	1.5-m
A-0298	Tiersch/Oliveira/MacGillivray/Böhringer	Structure and kinematics of Shakhbazian groups	1.5-m, 1.5-mD
B-0512	Tresse/Hammer/Rola/Stasinska	Spectral identification of faint blue galaxies in deep survey	NTT

ESO No.	Names of PIs (in alphabetical order)	Title of submitted programme	Telescope(s)
D-0478	Turatto/Benetti/Bouchet/Cappellaro/ Chugai/Della Valle/Danziger/Lucy/ Mazzali/Patà/Phillips	The evolution of SN events from the explosion to the remnant	1.5-m, 0.9-m Du
D-0689	Turon/Mermilliod/Gomez/Robichon/ Sellier/Guibert	Photometric calibration for open clusters observed with Hipparcos	0.9-m Du
B-0612	Ulrich/Molendi/Doublier	Spectroscopy of quasars with extreme α_{ox}	2.2-m
E-0777	van der Bliek/Schwarz/Nyman/Eriksson/ Gustafsson	Symbiotics: ancient mass transfer just like in Ba stars?	1.4-m CAT
C-0737	van der Hulst/de Graauw/van der Werf/ Israel/Baluteau/Joubert/Armand	Physical conditions of H II regions in the Magellanic Clouds	1.5-m
C-0185	van Hoof/Van de Steene/Pottasch	Accurate abundance determination of CNO in planetary nebulae	1.5-m
E-0567	van Loon/Loup/Trams/Waters/Zijlstra	Mass loss and AGB departure: population study in the LMC	2.2-m, 1.5-m D
D-0163	van Paradijs/Augusteijn/Abbott/ Leibundgut/Strom	Supernova light curves	0.9-m Du
D-0251	van Paradijs/Augusteijn/Kaper/Roche/ van der Klis/van Kerkwijk/Zuiderwijk	Weighing the neutron star in Vela X-1	1.4-m CAT
D-0651	van Paradijs/Charles/Casares/van der Hooft/van der Klis/Augusteijn	Black hole candidates in quiescent soft X-ray transients: spectroscopy	NTT
D-0647	van Paradijs/Charles/Casares/van der Hooft/van der Klis/Augusteijn	Black hole candidates in quiescent soft X-ray transients: photometry	1.5-m D
D-0589	van Teeseling/Reinsch/Beuermann/ Thomas/Pakull	The nature of supersoft X-ray sources	3.6-m
D-0592	Venn/Kudritzki/Lennon/Husfeld	Spectral analyses of A-type supergiants in the LMC: their evolutionary status and calibrating the wind momentum-luminosity relationship	3.6-m
B-0723	Vestergaard/Wilkes/Barthel	A torus in all quasars? Getting to the core of QSOs with broad emission lines	2.2-m
A-0546	Vigotti/Bardelli/Benn/Scaramella/ Vetolani/Zamorani/Zanichelli/Wall	Search and study of intermediate-redshift clusters by using radio sources as tracers	3.6-m
C-0799	Vladilo/Centurión	Calcium ionisation in Galactic halo gas	1.4-m CAT
D-0374	Waelkens/Aerts	Asteroseismology of slowly pulsating B stars	1.4-m CAT
B-0119	Wagner/Döbereiner	Near-IR mapping of the inner jet of Centaurus A	2.2-m
C-0455	Walsh/Ageorges	The 3-d form of the η Carinae nebula from high spatial resolution imaging polarimetry	3.6-m
A-0649	Warren/Hewett/Iovino/Møller/Shaver	An optical Einstein ring	NTT
D-0564	Waters/Zaal/Marlborough/Dougherty/ Taylor	Millimetre photometry of Be stars	SEST
D-0417	Waters/Zaal/Marlborough/Geballe	Br-alpha spectroscopy of OB stars	NTT
B-0678	Webb/Lanzetta/Barcons	Dynamics of galaxies to $\approx 160 h^{-1}$ kpc	NTT
E-0372	Weigelt/Davidson/Duschl/Geng/Kohl/ Langer/Scholz/Schöller/Reinheimer/ Seggewiss/Urban	Optical/IR speckle observations of evolved stars and their environment	3.6-m
F-0807	West/Hainaut/Marsden/Meech	Activity in very distant comets	NTT, 1.5-m D
E-0650	Westerlund/Azzopardi/Breysacher	Low-luminosity carbon stars in the Large Magellanic Cloud	2.2-m
B-0177	Wild/Wiklind	Dense molecular gas in Centaurus A	SEST
D-0258	Will/Seggewiss/Vázquez/Feinstein/ Schmidt	The initial mass function of the bright stars in IC 2602	1.5-m D
B-0606	Williger	Clustering in the early universe	NTT
C-0518	Wilson/Hüttemeister/Henkel	Sio in the Galactic centre region	SEST
B-0427	Wisotzki/Reimers/Köhler/Smette	Spectrophotometric monitoring of the double QSO He 1104–1805	3.6-m
D-0235	Wolf/Kaufer/Rivinius/Stahl/Gäng/ Gummersbach/Kovacs/Mandel/ Sterken/Szeifert	Luminosity dependence of mass-loss variations of early B-type stars	0.5-m
D-0167	Wolf/Kaufer/Stahl/Szeifert/Zickgraf	High-dispersion spectroscopy of luminous blue variables of the MCs	3.6-m
C-0630			SEST
C-0178	Yun/Clemens/Moreira	Gas structure and kinematics in filamentary dark clouds	3.6-m
B-0375	Yun/Moreira	Mid-infrared study of young stellar objects in Bok globules	3.6-m
A-0234	Zamorani/Giacconi/Hasinger/Marano/ Mignoli/Zitelli	Spectroscopic follow-up of ROSAT-discovered X-ray sources in the "Marano Field"	NTT
E-0565	Ziegler/Bender	The age of elliptical galaxies in clusters	NTT
E-0738	Zijlstra/Minniti	Miras in nearby galaxies (cont.)	1.5-m D
E-0681	Zijlstra/Van de Steene/van Loon/Loup/ Waters/te Lintel Hekkert	Long-period variables in the Blanco fields in the LMC	2.2-m
C-0670	Zijlstra/van Loon/Loup/Waters/ Whitelock	The AGB mass-loss function in the LMC	SEST
E-0519	Zinnecker/Brandner/Jung/Nürnberg/ Bronfman	Molecular line observations of the NGC 3603 GMC: evidence for sequential star formation?	3.6-m
	Zinnecker/Quirrenbach	Br γ and H ₂ imaging of pre-main sequence stars with infrared companions	

FIRST ANNOUNCEMENT

The Fourth CTIO/ESO Workshop

THE GALACTIC CENTER

10–15 March 1996, La Serena, CHILE

TOPICS

Infrared imaging and spectroscopy, millimeter and radio studies, radial velocity studies, Sgr A, annihilation source.

INVITED SPEAKERS

D. Aitken, J. Bally, M. Burton, T. Geballe, R. Genzel, D. Gezari, T. Herbst, P. Ho, P. Mezger, M. Morris, A. Omont, A. Sandquist, M. Rosa, H. Zinnecker.

CONTACT ADDRESSES

Roland Gredel and Jorge Melnick,
ESO, Casilla 19001, Santiago 19, Chile
(rgredel@eso.org); (jmelnick@eso.org)
Bob Schommer, CTIO, Casilla 603, La Serena, Chile
(schommer@ctiow7.ctio.noao.edu)

Time-table of Council and Committee Meetings (1995)

February 10	Scientific Technical Committee (extraord.)
March 21	Finance Committee (extraord.)
May 2–3	Users Committee
May 4–5	Scientific Technical Committee
May 9–10	Finance Committee
May 29 – June 1	Observing Programmes Committee
June 7–8	Council
September 25	Finance Committee (extraord.)
November 2–3	Scientific Technical Committee
November 6–7	Finance Committee
November 21–24	Observing Programmes Committee
November 28–29	Council

PERSONNEL MOVEMENTS

International staff (1 July – 30 Sept. 1995)

ARRIVALS

Europe

BELHACHEMI, Khadidja (F), Associate
BRAUNEIS, Wolfgang (A), Senior Personnel Officer
BRUCHMANN, Kathrin (D), Administrative Clerk (Personnel)
DA COSTA, Luiz (BR), Associate
DEVILLARD, Nicolas (F), Cooperant
ERM, Toomas (S), Electrical Engineer
JANDER, Georg (D), Mechanical Engineer
LEVEQUE, Samuel (F), Student
LUCY, Leon (GB), Associate
MENDEZ BUSSARD, René (RCH), Fellow
MÜLLER, Karen (SA), Student
QUINN, Peter (AUS), Head, Data Management Division
RENNZINI, Alvio (I), VLT Programme Scientist
SCHWARZ, Joseph (USA), Head of ADP Group
VEROLA, Massimo (I), Software Engineer

Chile

HAIKALA, Lauri (SF), Associate
LE MIGNANT, David (F), Student

TRANSFERS

KRETSCHMER, Gerhard (D), Mechanical Engineer
transferred from Garching to Chile

DEPARTURES

Europe

BEUZIT, Jean-Luc (F), Associate
PALMA, Francesco (I), Procurement Officer
SAHU, Kailash (IND), Associate

Chile

PERSSON, Glenn (S), Telescope Software Scientist
SCHWARZ, Hugo (NL), Astronomer

Local Staff Chile (1 Jan. – 30 Sept. 1995)

ARRIVALS

ABUTER, Roberto, Informatic Engineer (VLT)
AVILES, Roberto, Instruments Operator (Astronomy)
C. ARCOS, Juan, Warehouse Assistant (Administration)

CARRASCO, Marcelo, Computation Engineer (Astronomy)
ESPINOSA, Jorge, Optical Detector Specialist (TRS)
I. LEÓN, José, Informatic Engineer (VLT)
MARTÍN, Gabriel, Instruments Operator (Astronomy)
MUÑOZ, Ivan, Informatic Engineer (VLT)
NAVARRETE, Julio, Site Monitoring Assistant (VLT)
VILLAVUEVA, Raul, Civil Engineer VLT)

List of Preprints

(July–August 1995)

Scientific Preprints

1086. P. A. Mazzali and N. N. Chugai: Barium in SN 1987A and SNe II-P. *AA*.
1087. D. Minniti: Velocities of Supergiants in the Bulge of M33. *AA*.
1088. D. Minniti et al.: The Metallicity Gradient of the Galactic Bulge. *M.N.R.A.S.*
1089. E. Cappellaro, I.J. Danziger, M. Turatto: SN 1986E Eight Years After Outburst: a Link to SN 1957D? *M.N.R.A.S.*
1090. S. Serjeant, M. Lacy, S. Rawlings, L.J. King, D.L. Clements. Spectroscopic Evidence that the Extreme Properties of IRAS F 10214+4724 Are Due to Gravitational Lensing. *M.N.R.A.S.*
1091. W. Freudling and M.A. Prieto: Environment of Seyfert 2 Galaxies: the Group of Galaxies Around NGC 5252. *AA*.
1092. T.W. Berghöfer et al.: Correlated Variability in the X-Ray and H α Emission from the O4If Supergiant ζ Puppis. *AA*.
1093. X.-W. Liu, M.J. Barlow, I.J. Danziger, P.J. Storey: Balmer Discontinuity Temperatures in the Orion Nebula. *Ap. J. Letters*.
1094. M.-H. Ulrich and S. Molendi: The ROSAT-PSPC Spectrum of Bright Low z Quasars. *Ap. J.*
1095. S. Cristiani et al.: The Optical Variability of QSOs. *AA*.
1096. Bo Reipurth and R. Bachiller: CO Outflows from Young Stars. Invited Review presented at IAU Symposium 170. CO: Twenty-five Years of Millimeter-wave Spectroscopy, 29 May – 2 June 1995, Tucson, Arizona, USA.
1097. S. Hubrig and G. Mathys: Some Remarks on the Origin of the Abundance Anomalies in HgMn Stars. *Comments on Astrophysics*.
1098. D. Minniti, E.W. Olszewski, M. Rieke: IR Color-Magnitude Diagrams of 20 Galactic Globular Clusters and Bulge Fields. *A.J.*
1099. F. Patat and G. Carraro: NGC 7762: a Forgotten Moderate Age Open Cluster. *AA*.
1100. F. Patat et al.: The Type Ia SN 1994D in NGC 4526: The Early Phases. *M.N.R.A.S.*
1101. L. Pasquini and P. Molaro: Lithium Abundance in the Globular Cluster NGC 6397. *AA*.

Technical Preprint

68. O. von der Lühe et al.: Interferometry with the ESO Very Large Telescope.
S. Lévêque, B. Koehler, O. von der Lühe: Measurement of Optical Path Fluctuations Due to Internal Seeing for the VLT.
Optical Aperture Synthesis, SPIE Proceedings Vol. 2566, 1995.

ESO, the European Southern Observatory, was created in 1962 to . . . establish and operate an astronomical observatory in the southern hemisphere, equipped with powerful instruments, with the aim of furthering and organising collaboration in astronomy . . . It is supported by eight countries: Belgium, Denmark, France, Germany, Italy, the Netherlands, Sweden and Switzerland. It operates the La Silla observatory in the Atacama desert, 600 km north of Santiago de Chile, at 2,400 m altitude, where fourteen optical telescopes with diameters up to 3.6 m and a 15-m sub-millimetre radio telescope (SEST) are now in operation. The 3.5-m New Technology Telescope (NTT) became operational in 1990, and a giant telescope (VLT = Very Large Telescope), consisting of four 8-m telescopes (equivalent aperture = 16 m) is under construction. It is being erected on Paranal, a 2,600 m high mountain in northern Chile, approximately 130 km south of Antofagasta. Eight hundred scientists make proposals each year for the use of the telescopes at La Silla. The ESO Headquarters are located in Garching, near Munich, Germany. It is the scientific-technical and administrative centre of ESO where technical development programmes are carried out to provide the La Silla observatory with the most advanced instruments. There are also extensive facilities which enable the scientists to analyse their data. In Europe ESO employs about 200 international Staff members, Fellows and Associates; at La Silla about 50 and, in addition, 150 local Staff members.

The ESO MESSENGER is published four times a year: normally in March, June, September and December. ESO also publishes Conference Proceedings, Preprints, Technical Notes and other material connected to its activities. Press Releases inform the media about particular events. For further information, contact the ESO Information Service at the following address:

EUROPEAN
SOUTHERN OBSERVATORY
Karl-Schwarzschild-Str. 2
D-85748 Garching bei München
Germany
Tel. (089) 320 06-0
Telex 5-28282-0 eo d
Telefax (089) 3202362
ips@eso.org (internet)
ESO::IPS (decnet)

The ESO Messenger:
Editor: Marie-Hélène Demoulin
Technical editor: Kurt Kjær

Printed by Universitäts-Druckerei
Dr. C. Wolf & Sohn
Heidemannstraße 166
D-80939 München 45
Germany
ISSN 0722-6691

Last Copies of ESO/SRC Atlas Available

A few complete copies of the ESO/SRC Atlas are still available from ESO. The price of one Atlas, comprising a total of 1212 on-film copies of J and R exposures made with the UK and ESO Schmidts, respectively, and showing the sky south of declination $-17^{\circ}5$ to limiting magnitude 22–23, is DM 24,000, including postal charges. No further editions will ever be made of this Atlas.

Orders will be accepted until January 15, 1996. Please contact:

ESO Information Service
Karl-Schwarzschild-Str. 2
D-85748 Garching
Germany

Tel.: +4989-32006-276; Fax.: +4989-3202362

Contents

TELESCOPES AND INSTRUMENTATION

M. Tarenghi: News from Paranal and Current Status of VLT Construction Work	1
C. Madsen: ESO Donates DM 100,000 For Reconstruction Work After Earthquake in Northern Chile	3
D. Enard: News from the Secondary Mirror Units	3
G. Raffi: The VLT Control Software — Status Report	5
T. Herlin, A. Brighton, P. Biereichel: The VLT Real Time Display Software	6
NTT Bits and Pixels	8

Additional News from the La Silla Site

L. Pasquini and L. Achmad: CASPEC Thorium-Argon Atlas in the 3050—3650 Å Region	9
H. Schwarz and S. Guisard: Rotating Half Wave Plate for EFOSC1 Refurbished	9
C. Lidman: Superb Seeing on the 2.2-m Telescope with IRAS2	10
Photometry with EFOSC2	10
C. Oliveira: New Autoguider at the 1.52-m	10
J. Mendez: Satellite Pictures Available in the "Meteomonitor" Environment	10
G. Ihle: The Last Trip of the ESO GPO	10
R. West: A Spectacular Jet in Comet Hale-Bopp	11

REPORTS FROM OBSERVERS

J.P.E. Gerritsen and P.D. Barthel: Near-Infrared Imaging of QSO Host Galaxies	12
D. Macchetto and M. Giavalisco: Have We Detected the Primeval Galaxies?	14
B. Leibundgut et al.: Discovery of a Supernova (SN 1995K) at a Redshift of 0.478	19
K.S. de Boer, H.-J. Ticholke, W.C. Seitter: The Magellanic Catalogue of Stars — MACS	20

OTHER ASTRONOMICAL NEWS

A.A. Zijlstra, J. Rodriguez, A. Wallander: Remote Observing and Experience at ESO	23
U. Grothkopf, F. Murtagh, M. Albrecht: Library and Information Services in Astronomy II (LISA-II)	27

ANNOUNCEMENTS

Programmes Approved for Period 56	29
Fourth CTIO/ESO Workshop	35
Tentative Time-table of Council and Committee Meetings	35
Personnel Movements	35
New ESO Preprints	35
Last Copies of ESO/SRC Atlas Available	36